

Allogenic sedimentary components of Bear Lake, Utah and Idaho

Joseph G. Rosenbaum
Walter E. Dean
Richard L. Reynolds
Marith C. Reheis

U.S. Geological Survey, Box 25046, Federal Center, Denver, Colorado 80225, USA

ABSTRACT

Bear Lake is a long-lived lake filling a tectonic depression between the Bear River Range to the west and the Bear River Plateau to the east, and straddling the border between Utah and Idaho. Mineralogy, elemental geochemistry, and magnetic properties provide information about variations in provenance of allogenic lithic material in last-glacial-age, quartz-rich sediment in Bear Lake. Grain-size data from the siliclastic fraction of late-glacial to Holocene carbonate-rich sediments provide information about variations in lake level. For the quartz-rich lower unit, which was deposited while the Bear River flowed into and out of the lake, four source areas are recognized on the basis of modern fluvial samples with contrasting properties that reflect differences in bedrock geology and in magnetite content from dust. One of these areas is underlain by hematite-rich Uinta Mountain Group rocks in the headwaters of the Bear River. Although Uinta Mountain Group rocks make up a small fraction of the catchment, hematite-rich material from this area is an important component of the lower unit. This material is interpreted to be glacial flour. Variations in the input of glacial flour are interpreted as having caused quasi-cyclical variations in mineralogical and elemental concentrations, and in magnetic properties within the lower unit. The carbonate-rich younger unit was deposited under conditions similar to those of the modern lake, with the Bear River largely bypassing the lake. For two cores taken in more than 30 m of water, median grain sizes in this unit range from ~6 μm to more than 30 μm , with the coarsest grain sizes associated with beach or shallow-water deposits. Similar grain-size variations are observed as a function of water depth in the modern lake and provide the basis for interpreting the core grain-size data in terms of lake level.

INTRODUCTION

Bear Lake Valley, on the border between Utah and Idaho, is formed by a tectonically active half-graben (Colman, 2006; Reheis et al., this volume) between the Bear River Range to the west and the Bear Lake Plateau to the east (Fig. 1). The southern part of the

valley is occupied by Bear Lake, which is ~32 km long, 6–13 km wide, and 63 m deep. The Bear River flows into the valley north of the lake. During historic times the river did not enter the lake until it was diverted ca. 1912 (Dean et al., this volume) but did flow into the lake at various times during the late Pleistocene (Kaufman et al., this volume; Reheis et al., this volume).

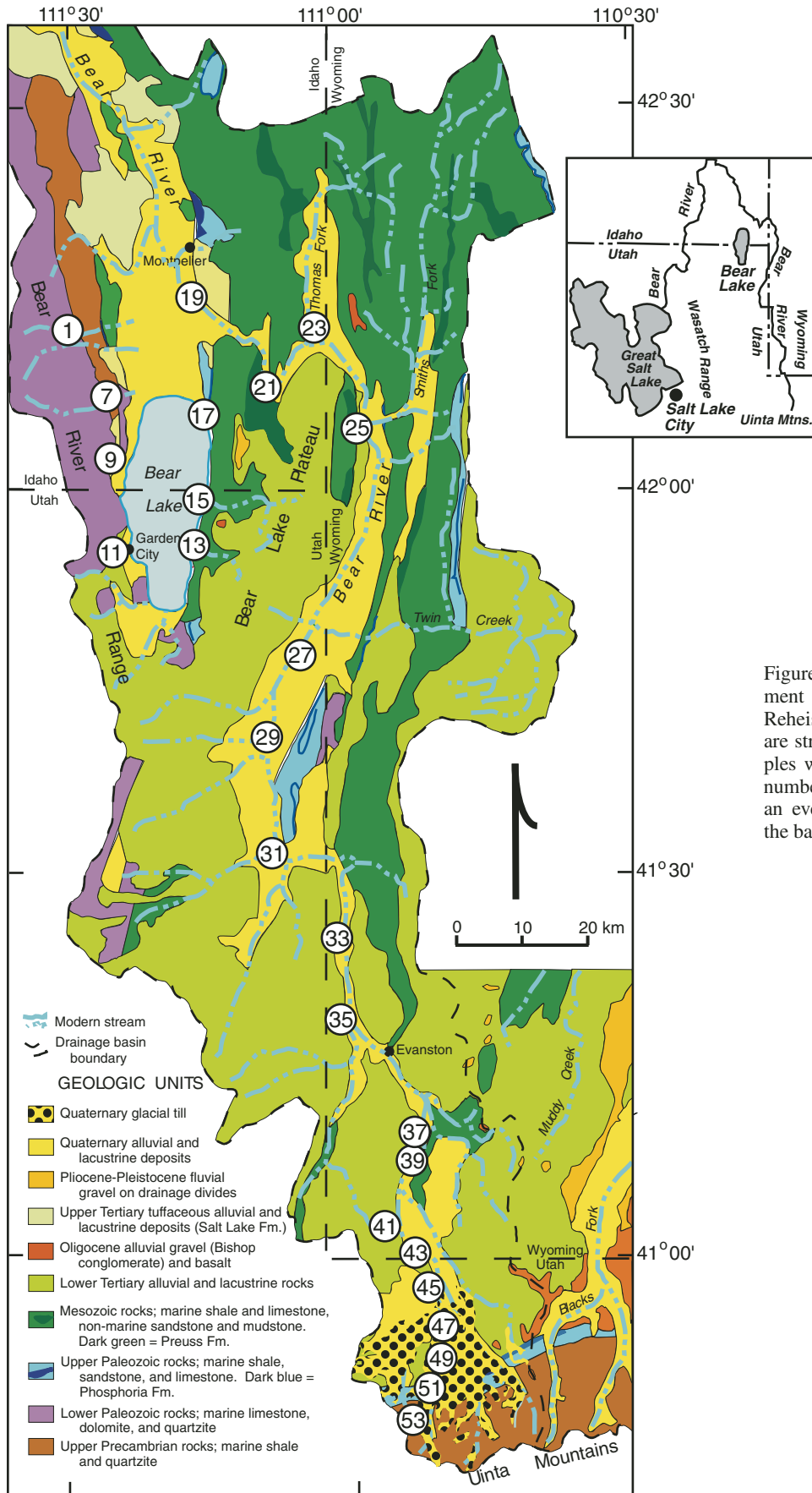


Figure 1. Generalized geologic map of catchment areas for Bear Lake (modified from Reheis et al., this volume). Numbered circles are stream sediment sampling sites. Two samples were collected at each location, an odd-numbered sample from the stream bottom and an even-numbered sample (not shown) from the bank or the overbank deposit.

In the absence of the Bear River, surface flow into Bear Lake is from a number of streams in a small drainage basin. This "local" catchment can be divided into two parts on the basis of bedrock geology (Oriol and Platt, 1980; Dover, 1995). The Bear River Range to the west of the lake is largely underlain by lower Paleozoic formations containing large amounts of dolomite, quartzite, and limestone, with lesser amounts of Precambrian quartzite and shale, as well as clastic Tertiary rocks of the Wasatch Formation. Rocks constituting the Bear Lake Plateau on the east side of the lake consist of abundant Tertiary Wasatch Formation and Mesozoic limestone and clastic sedimentary rocks.

When the Bear River flows into Bear Lake the lake's catchment is much larger. Bedrock along most of the Bear River upstream from Bear Lake is similar to that in the Bear River Plateau, with widespread Tertiary and Mesozoic sedimentary rocks. Bedrock in the river's headwaters, however, comprises Precambrian quartzites and shales of the Uinta Mountain Group (Bryant, 1992).

Bear Lake sediments contain both endogenic and allogenic components. The endogenic component, which consists of minerals formed in the water column and the remains of biota that grew in the lake, directly reflects physical and chemical conditions of the lake. In contrast, allogenic components, which are transported to the lake by water and wind, largely reflect catchment conditions and processes. Some allogenic components may be affected by post-depositional alteration and thereby in part reflect lake conditions rather than catchment conditions.

Here we report data that largely reflect the allogenic component of Bear Lake sediments as well as data from the potential source areas of this component. The data derived by individual techniques, however, do not separate cleanly into groupings that yield information about solely endogenic or solely allogenic materials. For instance, X-ray diffraction data for the lake sediments reported by Dean (this volume), contain information about endogenic carbonate minerals (e.g., calcite and aragonite) as well as information about allogenic minerals (e.g., quartz, calcite, and dolomite). Data from lake sediments presented here (elemental geochemistry on bulk samples, magnetic properties, and grain size of the siliciclastic material) primarily provide information about material derived from the catchment and secondarily about processes within the lake. The bulk-sample elemental data reflect the contents of both carbonate and siliciclastic minerals. Additional elemental data reported by Bischoff et al. (2005) and Dean (this volume), which were acquired from the HCl-soluble component, largely reflect the carbonate minerals of both endogenic and detrital origins. Magnetic properties reflect not only the detrital minerals delivered to the lake but also the effects of post-depositional processes that commonly destroy Fe-oxide minerals or form secondary magnetic phases. Similarly, grain-size distributions of siliciclastic detrital material are affected not only by the sizes of material delivered to the lake but also by sorting during settling and resuspension within the lake.

The large volume of data reported herein contributes to a number of important interpretations presented in other chapters of this volume. For example, (1) variations in mineralogy and

magnetic properties are used to correlate stratigraphic horizons among cores (Colman et al., this volume); (2) mineralogical data indicative of provenance help establish the presence or absence of Bear River input to the lake (Kaufman et al., this volume); (3) grain-size data contribute to the interpretation of lake-level history (Smoot and Rosenbaum, this volume); and (4) magnetic property, mineralogical, geochemical, and grain-size data provide the basis for a glacial history based on glacial flour in the lake sediments (Rosenbaum and Heil, this volume).

METHODS

Sampling

Fluvial Sediment

Streams draining the Bear River Range and the Bear River Plateau, as well as the Bear River are potential sources of fluvial input to Bear Lake (Fig. 1). Because environmental change can alter the amounts of material derived from areas of different bedrock lithologies, such change may be reflected in the mineralogical, chemical, and physical properties of lithic materials in the lake sediments. Characterization of materials from different parts of the drainage basins can help constrain interpretations of environmental change based on data obtained from lake-sediment cores.

Samples of fluvial material were collected from (1) streams draining the east and west sides of the local Bear Lake catchment and (2) the Bear River upstream from Bear Lake (Fig. 1). Two samples were taken at each site, an odd-numbered sample from the stream bottom and an even-numbered sample from the stream bank or overbank deposit. The samples, which include all grain sizes up to a few centimeters in diameter, integrate lithologies upstream from the sampling sites. The samples were sieved into four grain-size ranges: pebbles (2 mm to several cm), coarse sand and granules (0.42 mm to ~2 mm), fine and medium sand (0.053 mm to 0.42 mm), and silt and clay (less than 0.053 mm). The pebble fractions were coarsely crushed so that small splits of these fractions represent a mixture of the lithologies present in the samples. Splits were taken from the size fractions for a variety of measurements, which are described below.

Dust

Dust traps were constructed at three sites within 10 m of the shoreline of Bear Lake (Fig. 2) to sample the annual vertical dust deposition to the lake area. Sites were located on the fan of South Eden Creek (BL-1), just south of Garden City (BL-2), and near the Lifton pump station (BL-3). The dust traps were established in 1998 and sampled annually in 1999 and 2000. The dust-trap design is that described by Reheis and Kihl (1995) and yields samples that include both wet and dry dust deposition. Laboratory analyses followed procedure described in Reheis (2003).

Lake Sediment

Lake sediments were cored (Fig. 2) using a variety of devices (Rosenbaum and Kaufman, this volume). Short cores, as much as a

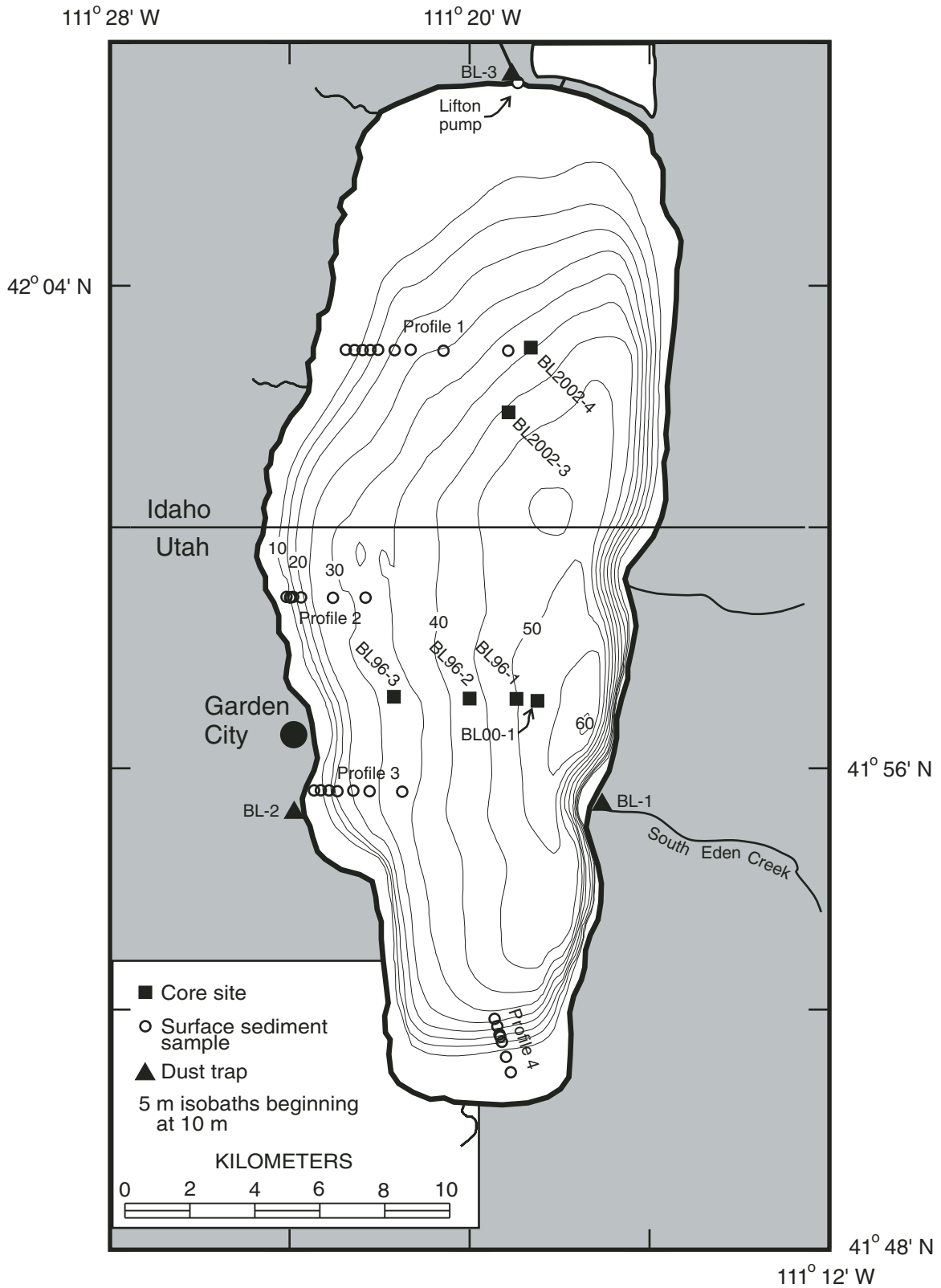


Figure 2. Map of Bear Lake showing bathymetry (Denny and Colman, 2003) and locations of cores, dust traps, and surface sediment samples.

few tens of centimeters in length, preserved the uppermost unconsolidated sediments. The sampling interval was typically 1 cm, but surface samples, which were taken with the same coring device, are 1.5 cm thick. Longer cores, which penetrated up to 5 m of sediment, were collected in plastic liners. These cores were split lengthwise, with one-half of each core being preserved and logged (Smoot, this volume) and the other half being cut into samples at 1 cm intervals. Samples were then subdivided for a variety of analyses.

Analyses

Major minerals and elemental concentrations were determined for lake-sediment samples and for the silt-and-clay and coarse-sand fractions of fluvial sediment. Standard X-ray diffraction techniques were used for mineral identification (e.g., Moore and Reynolds, 1989). Powdered samples were packed into aluminum holders and scanned from 15° to 50° using Ni-filtered, Cu-K α radiation. Semiquantitative mineral contents were determined by normalizing the major peak intensity of a mineral by the sum of major peak intensities for all minerals. This method does not account for differences in the X-ray absorption characteristics of individual minerals; nevertheless, these values provide excellent relative values for sample-to-sample comparison as long as the minerals in the samples are similar. The lake-sediment X-ray data are reported by Dean (this volume). Elemental concentrations were determined by XRAL Laboratories (Toronto, Canada) using Inductively Coupled Plasma-Atomic Emission Spectrometry following digestion of powdered samples in a combination of hydrochloric, nitric, hydrofluoric, and perchloric acids.

For magnetic property analyses, samples of lake sediments and of all four size fractions of fluvial material were packed in nonmagnetic 3.2 cm³ plastic boxes. The analyses include measurements of magnetic susceptibility (MS), anhysteretic remanent magnetization (ARM), and isothermal remanent magnetization (IRM). ARM and IRM were measured with a high-speed spinner magnetometer. ARM was imparted using an alternating field with a peak intensity of 0.1 Tesla (T) and a bias field of 0.1 milliTesla (mT). After measurement of ARM, IRM was first imparted in a 1.2 T field (IRM_{1.2T}) and then in the opposite direction in a field of 0.3 T (IRM_{-0.3T}). Hard isothermal remanent magnetization (HIRM) and the S-parameter (King and Channel, 1991) are given by:

$$\text{HIRM} = (\text{IRM}_{1.2\text{T}} - \text{IRM}_{-0.3\text{T}})/2, \quad (1)$$

and

$$S = \text{IRM}_{-0.3\text{T}}/\text{IRM}_{1.2\text{T}}. \quad (2)$$

Samples then were dried and weighed. MS values, which were acquired after drying to eliminate the diamagnetic effects of pore water, were measured in a 600 Hz alternating field with amplitude of ~0.1 mT. The MS readings were corrected for the diamagnetic effect of sample boxes. Dry bulk densities were cal-

culated by dividing the dry mass of each sample by the standard volume of the sample boxes (3.2 cm³).

For selected samples, magnetic minerals were concentrated using a separator described by Reynolds et al. (2001). For cores BL96-1, -2, and -3, samples were chosen to represent magnetic-property variations. In order to obtain enough material for analysis, most separates incorporated material from two or more closely spaced samples with similar magnetic properties. The separates were mounted in epoxy, polished, and then observed with reflected-light microscopy (Reynolds and Rosenbaum, 2005). In this manner, magnetic minerals were identified from 22 horizons. In addition, five separates were prepared from the silt and clay fraction of fluvial sediments. Most of these separates included material from multiple spatially related sites with similar magnetic properties.

Sample splits for grain-size analyses were treated sequentially with HCl, H₂O₂, and Na₂CO₃, to remove carbonate, organic matter, and opaline silica, respectively. A laser particle size analyzer, capable of measuring particles ranging from 0.49 to 2000 μm , was used to determine grain-size distributions on the residual siliciclastic material.

RESULTS

Fluvial Sediments

The mineralogical, elemental, and magnetic properties of fluvial sediment vary with grain size and location (Table 1, Figs. 3–5). The samples were divided geographically into four groups. Samples from streams in the local Bear Lake catchment were divided into those from the west side and those from the east side of the lake (Fig. 1). The Bear River samples were assigned to lower (samples 19 through 46) and upper (47 through 54) river groups based on properties described below.

Mineralogy and Elemental Chemistry

In comparison to Bear River sediments, samples from the local catchment are characterized by lower average quartz content and higher contents of carbonate minerals (Table 1, Fig. 3). Calcite is most abundant in samples from the east side of the lake, whereas high concentrations of dolomite are restricted to samples from the west side. These differences, which reflect bedrock geology (Fig. 1), are mirrored in the concentrations of Ca and Mg (Fig. 4). Concentrations of Ca are relatively high within the local catchment, and high values of Mg are restricted to the west-side samples. The between-sample variability of mineral and elemental contents is greater for the local catchment than for the Bear River. The higher variability of the local catchment samples probably reflects contrasting bedrock among the separate areas drained by the small streams. The lower variability of the Bear River samples is attributed to dilution of local bedrock material by a relatively homogeneous mixture of lithologies derived from large areas upstream of each sampling site.

The coarse fraction of Bear River sediments displays little variation in major minerals, although samples 19–29 contain

TABLE 1. AVERAGES OF MINERAL ABUNDANCES, ELEMENTAL ABUNDANCES, MAGNETIC SUSCEPTIBILITY, AND HARD ISOTHERMAL REMANENT MAGNETIZATION OF SILT-AND-CLAY FRACTION (S&C) AND COARSE-SAND FRACTION (CS) OF FLUVIAL SEDIMENT SAMPLES

	Size fraction	Quartz (%)	Calcite (%)	Dolomite (%)	Feldspar (%)	Al (%)	Ti (%)	Ca (%)	Mg (%)	MS x 10 ⁻⁷ (m ³ kg ⁻¹)	HIRM x 10 ⁻⁴ (Am ² kg ⁻¹)
Bear River	S&C	78	11	4	6	5.2	0.22	4.4	1.14	1.80	4.43
	CS	84	3	1	7	2.3	0.08	2.0	0.36	0.67	3.06
Lower	S&C	77	12	5	5	4.6	0.21	5.4	1.21	1.82	3.38
	CS	88	12	1	7	2.3	0.09	2.5	0.44	0.81	2.64
Upper	S&C	85	0	0	14	7.3	0.25	0.8	0.91	1.71	8.12
	CS	90	1	0	9	2.4	0.04	0.1	0.11	0.21	4.46
Local catchment	S&C	69	10	13	7	3.7	0.21	6.0	1.80	5.63	3.47
	CS	64	22	10	4	2.6	0.12	9.7	1.70	3.03	2.90
West side	S&C	67	4	21	8	3.6	0.21	5.5	2.37	6.09	3.43
	CS	69	13	14	4	2.7	0.13	7.9	2.21	3.23	3.08
East side	S&C	71	20	3	6	3.9	0.21	7.0	0.87	5.03	3.52
	CS	55	40	2	4	2.3	0.11	13.4	0.68	2.76	2.66

more calcite and slightly less quartz than samples from farther upstream (Fig. 3). This downstream increase in calcite, which is clearly reflected in the Ca concentrations, probably reflects greater input from the limestone-bearing Mesozoic bedrock (Fig. 1). The fine fraction of Bear River sediments contains less quartz and more calcite than the coarse fraction, suggesting that the coarse fraction is derived largely from sandstones and quartzites and the fine fraction is derived largely from more friable lithologies. This difference in lithologies is reflected in the contents of Al and Ti.

Moving upstream along the Bear River, both Al and Ti increase in the fine fraction and decrease in the coarse fraction (Fig. 4). In both fractions, Ti:Al decreases upriver, reaching minimum values in the headwaters in the Uinta Mountains.

Very high values of Mg:Ca in the uppermost reaches of the Bear River reflect the absence of carbonate bedrock, whereas elevated values of this ratio from the west side of the local catchment reflect abundant dolomite. The abundance of dolomite is more clearly reflected in the ratio of Mg to the chemically immobile

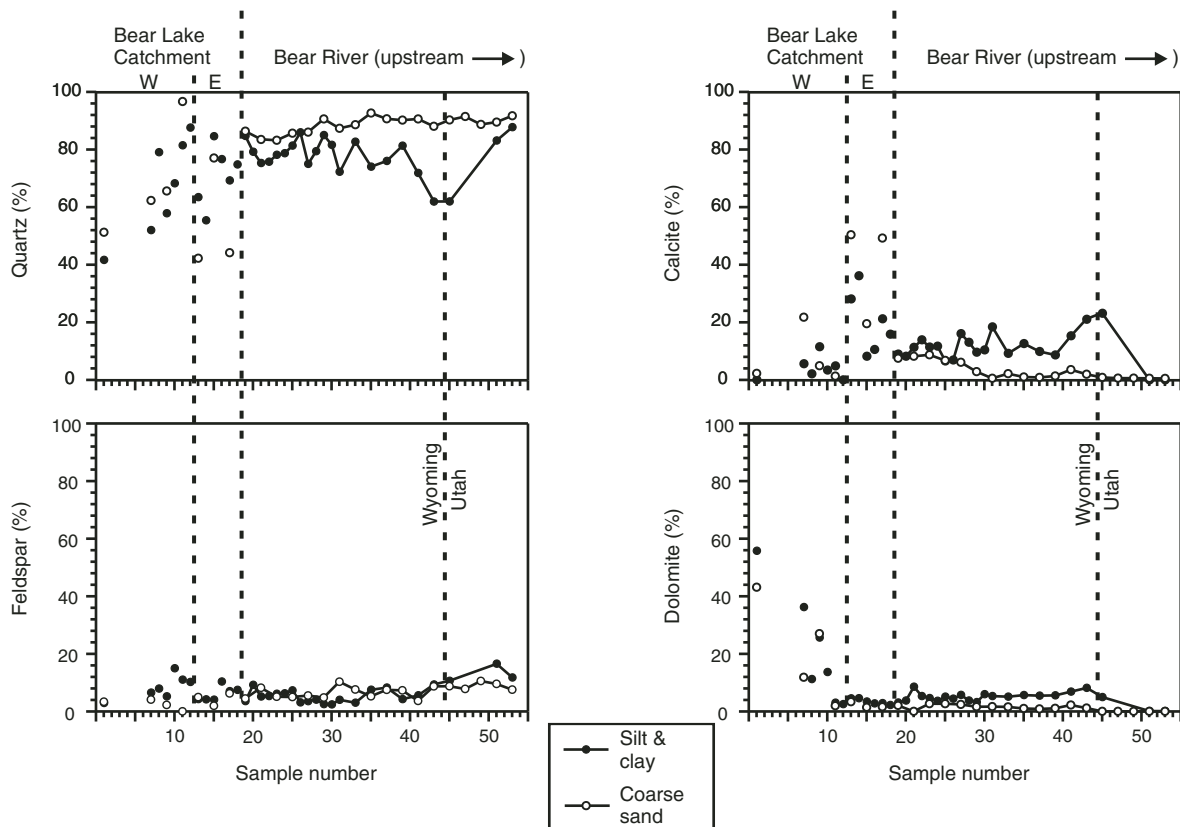


Figure 3. Contents of quartz, calcite, feldspar, and dolomite in two size fractions of fluvial sediment samples as determined by X-ray diffraction. Sample locations shown in Figure 1. Vertical dashed lines separate four catchment areas: west (W) and east (E) sides of the local catchment and the lower and upper Bear River.

element, Al (Fig. 4), which is delivered to the lake in aluminosilicate minerals.

Magnetic Properties

Magnetic properties provide strong contrasts among the four fluvial sediment groups (Table 1, Fig. 5). MS, which provides a measure of the content of ferrimagnetic minerals (e.g., magnetite, titanomagnetite, and maghemite), and HIRM, largely a measure

of hematite, do not covary. Values of MS for the silt-and-clay fraction of all sediment groups are higher than corresponding values from the coarser fractions. For the local Bear Lake catchment, MS values are relatively high and HIRM values are relatively low. In comparison to the local catchment, the lower Bear River group has lower MS values and similar HIRM values. Values of MS generally decrease upriver, whereas HIRM values increase upriver into the Uinta Mountains. Values of HIRM for

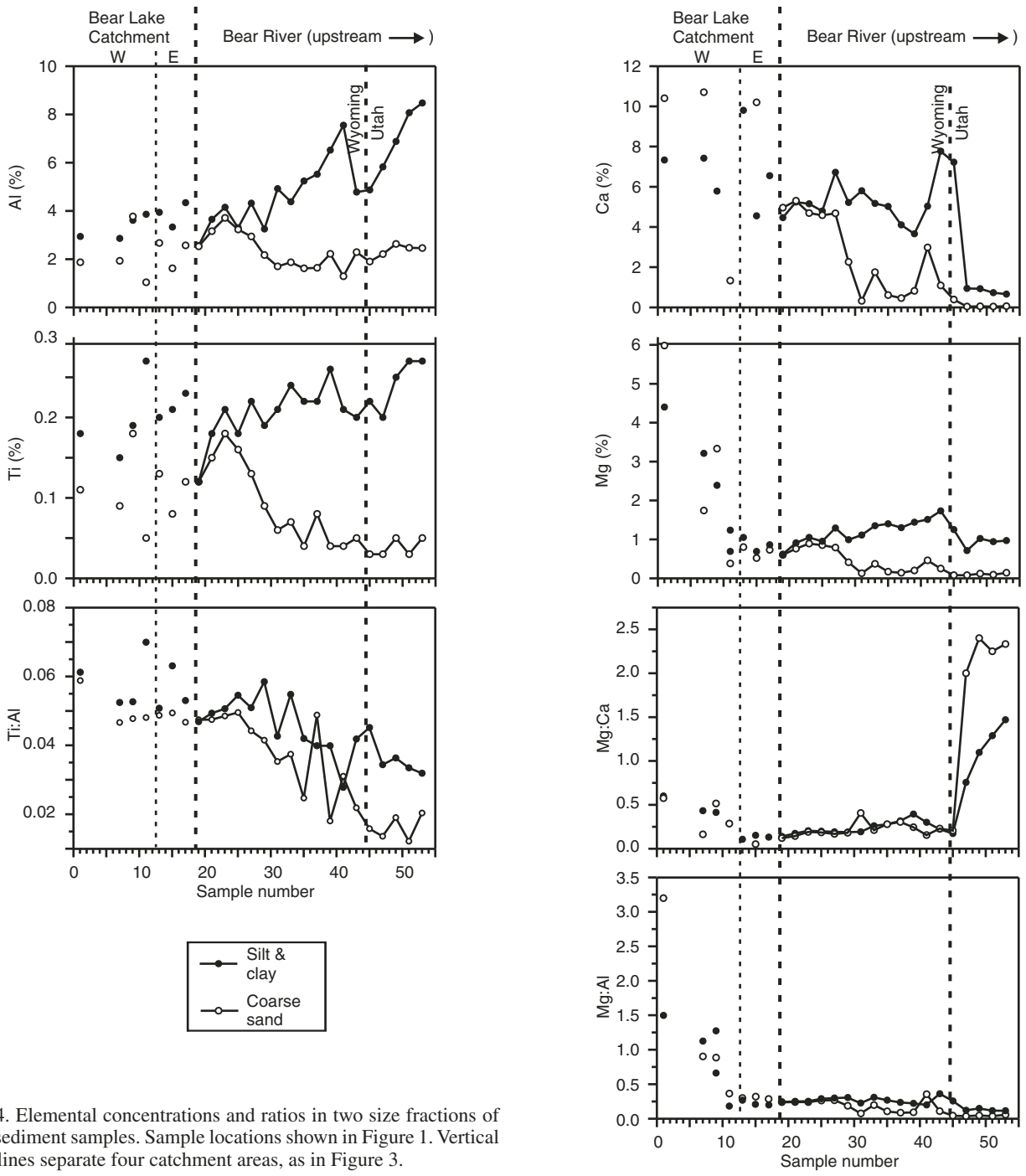


Figure 4. Elemental concentrations and ratios in two size fractions of stream sediment samples. Sample locations shown in Figure 1. Vertical dashed lines separate four catchment areas, as in Figure 3.

the silt-and-clay fraction from the upper Bear River are more than twice the values from the other areas.

Petrographic observations show that magnetite, which occurs commonly as mineral grains and less commonly within rock fragments, is the most abundant mineral in each of the magnetic separates (Reynolds and Rosenbaum, 2005). The magne-

tite occurs in a variety of forms, including homogeneous grains and titanomagnetite grains in which the magnetite is subdivided by ilmenite lamellae. Many of these grains formed under high-temperature conditions in igneous or metamorphic rocks. Ferri-magnetic titanohematite and hematite also occur in all samples. Like magnetite, hematite occurs in a variety of forms including

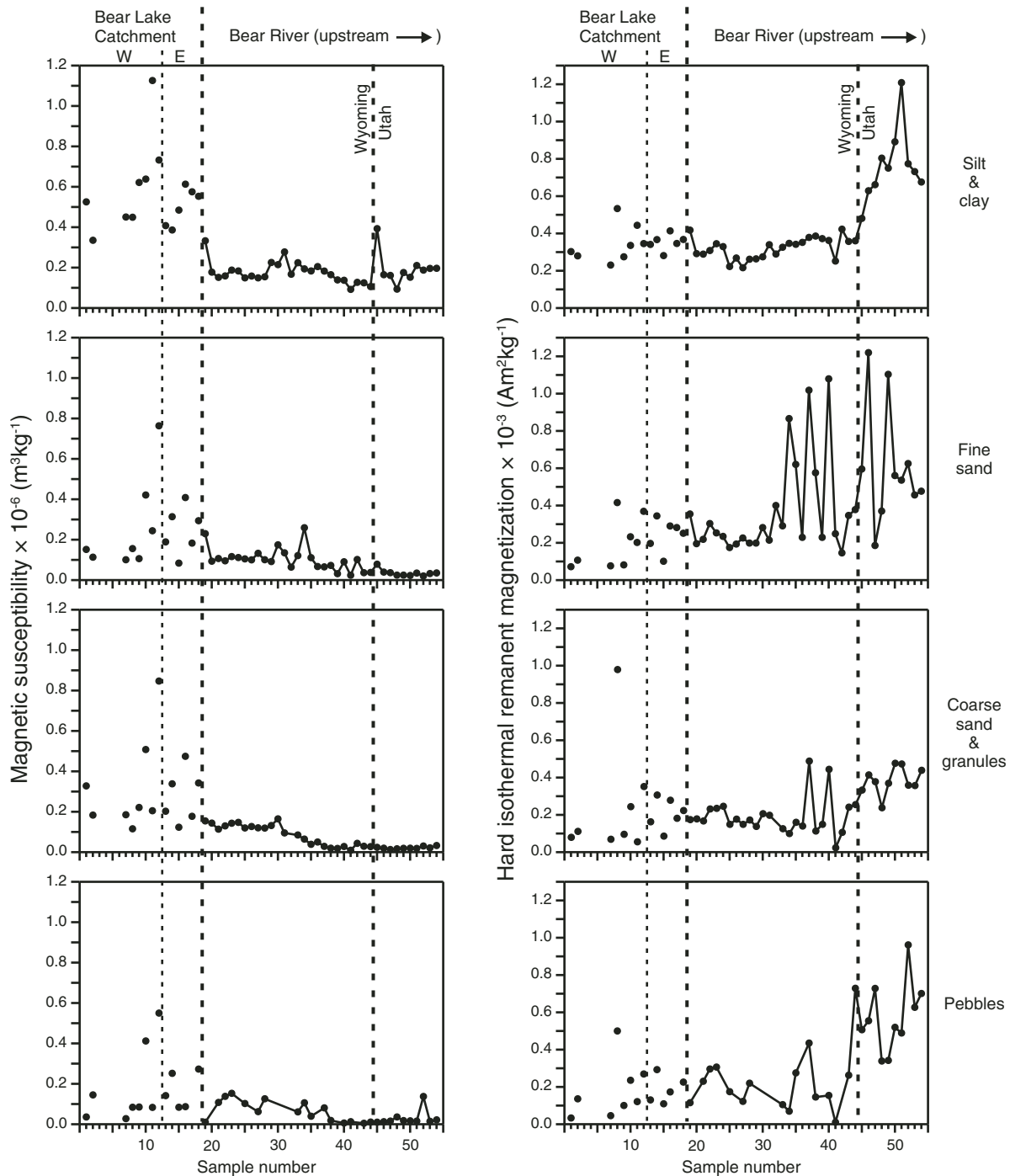


Figure 5. Magnetic susceptibility and hard isothermal remanent magnetization of four size fractions of stream sediment samples. Sample locations shown in Figure 1. Vertical dashed lines separate four catchment areas, as in Figure 3.

specular hematite and fine-grained forms. Some of the specular hematite occurs within titaniferous oxides that formed under high-temperature oxidizing conditions (e.g., pseudobrookite), whereas much of the fine-grained hematite occurs in rock fragments (e.g., red sedimentary rocks) and formed under low-temperature conditions. Red sedimentary rock fragments are particularly abundant in samples from the upper reaches of the Bear River (sites 48 and 51 in Fig. 1). In addition, most of the separates contain small quantities of anthropogenic material including fly ash and steel.

The magnetic grains are characterized by small sizes. Although the silt-and-clay size fraction used for the magnetic separates contains grains as large as 53 μm , few magnetic grains are $>20 \mu\text{m}$, and most are $<10 \mu\text{m}$.

Dust

The amounts, composition, and grain size of material collected in dust traps near Bear Lake vary between the two years of collection. The flux of total mineral matter ranges from ~ 5.5 to $>17 \text{ g m}^{-2} \text{ yr}^{-1}$ (Table 2). Much of this variation is produced by variations in sand content. The flux of the $<50 \mu\text{m}$ fraction averages $\sim 5 \text{ g m}^{-2} \text{ yr}^{-1}$ and is less variable. The CaCO_3 component of the dust flux is relatively low ($<1 \text{ g m}^{-2} \text{ yr}^{-1}$) and XRD analysis of dust samples indicates that more than 85% of the detritus consists of non-carbonate minerals, mainly quartz ($\sim 70\%$) and plagioclase with minor amounts of clays (G. Skipp, 2004, personal commun.). Concentrations of both salts and carbonate minerals are higher in the 1999–2000 samples than in the 1998–1999 samples (Table 2). These differences are due in large part to the much higher concentrations of sand (which is presumably quartz rich) in the earlier samples. In fact the fluxes of salt are very similar during the two sampling intervals and the fluxes of carbonate minerals are actually slightly lower during the second year.

Lake Sediments

Mineralogy

Sediments deposited over the last 26 k.y. consist of a quartz-rich lower unit and a carbonate-rich upper unit (Dean et al.,

2006; Dean, this volume; Smoot, this volume). Sediments in cores BL96-1 and BL2002-3 are entirely within the upper unit, whereas the transition between the two units occurs at $\sim 3, 0.4,$ and 3.3 m in cores BL96-2, BL96-3, and BL2002-4, respectively (Figs. 6–10). The carbonate-rich upper unit can be divided into four intervals on the basis of carbonate mineralogy (Dean et al., this volume). In ascending order these are a lower calcite interval, a lower aragonite interval, an upper calcite interval, and an upper aragonite interval.

Quartz content is $\sim 70\%$ in the lower unit and quite uniform. Quartz content in the upper, carbonate-rich unit is generally 20% to 30% with small but well-defined variations. Calcite content in the lower unit is typically between 10% and 20%. Within this unit, the majority of calcite is probably detrital but some may be endogenic. Calcite contents in the aragonite-rich intervals of the upper unit are similar to those in the quartz-rich unit. Within these intervals, much of the calcite may be detrital. The content of dolomite, which is also detrital, is generally between 8% and 9% in the lower unit and between 5% and 8% in the upper unit. Because the sensitivity of the XRD method is limited to a few percent, the dolomite curves are quite noisy; nevertheless, it is apparent that most changes in quartz and dolomite are synchronous. Although the contents of quartz and dolomite generally change at the same time, the dolomite-quartz ratio (Dolo:Qtz) is not constant. Dolo:Qtz increases slightly across the transition from the lower to the upper unit. Within the upper unit, Dolo:Qtz undergoes larger variations that roughly coincide with changes in carbonate mineralogy. Values of Dolo:Qtz are mostly low in the calcite-rich intervals and high in the lower aragonite-rich interval. Values rise in the upper aragonite-rich interval and then fall toward the upper part of the section.

Mass accumulation rates vary widely among the core sites (Table 3). In the quartz-rich lower unit comparison of accumulation rates among sites may not be meaningful because the cores span very different time intervals. For the carbonate-rich upper unit, average mass accumulation rates of both the carbonate and non-carbonate fractions generally increase with water depth. The ratio of carbonate to non-carbonate material also increases with water depth.

TABLE 2. DUST DATA FROM BEAR LAKE, 1998–2000

Trap no.*	OC (%) [†]	CaCO ₃ (total %)	Salts (total %)	Mineral wt. (g) [‡]	Percent of <2 mm fraction				Dust flux (g m ⁻² yr ⁻¹)	CaCO ₃ flux (g m ⁻² yr ⁻¹)	Salt flux (g m ⁻² yr ⁻¹)	Flux, g m ⁻² yr ⁻¹ (incl. CaCO ₃)				
					sand	silt	clay	<20 μm				sand	silt	clay	<20 μm	<50 μm
1998–1999																
BL-1	21.6	4.18	8.15	1.40	15.87	61.70	22.44	48.65	8.77	0.51	1.14	1.21	4.71	1.71	3.71	6.42
BL-2	19.0	4.40	3.64	2.61	72.73	25.13	2.14	9.76	17.60	1.09	0.95	12.11	4.18	0.36	1.62	4.54
BL-3	26.7	4.49	5.10	1.48	31.76	56.10	12.14	33.42	8.01	0.60	0.76	2.30	4.07	0.88	2.42	4.95
1999–2000																
BL-1	11.8	7.17	13.98	0.68	3.31	57.91	38.79	84.27	5.92	0.44	1.04	0.16	2.83	1.89	4.11	4.72
BL-2	18.2	7.25	12.83	0.73	7.45	63.86	28.69	71.82	5.46	0.47	1.02	0.33	2.83	1.27	3.19	4.11
BL-3	21.4	3.33	9.82	1.09	1.65	53.89	44.46	87.50	7.51	0.34	1.17	0.10	3.42	2.82	5.55	6.23

*BL-1, South Eden Creek adjacent to east shore of lake; BL-2, on breakwater at Bear Lake field station on southwest shore of lake; BL-3, on breakwater east of Lifton pump station on north shore of lake.

[†]OC—organic carbon.

[‡]Mineral weight excludes organic-matter content.

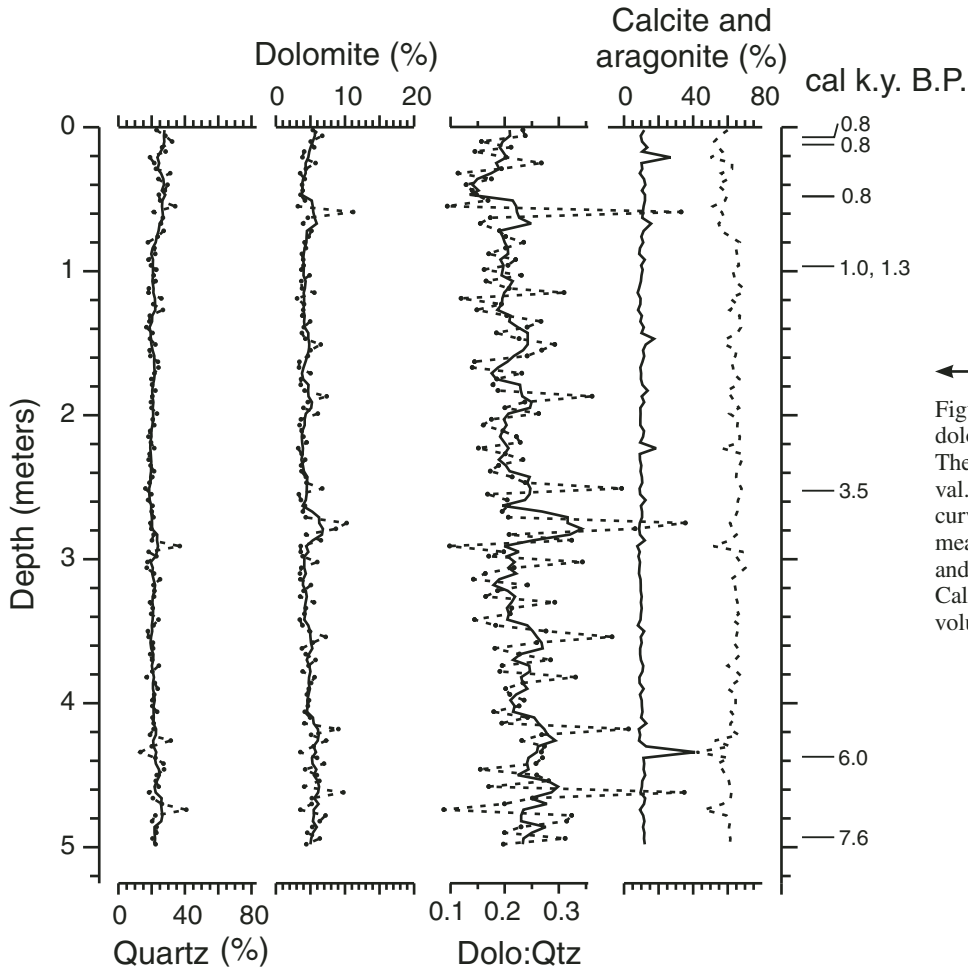
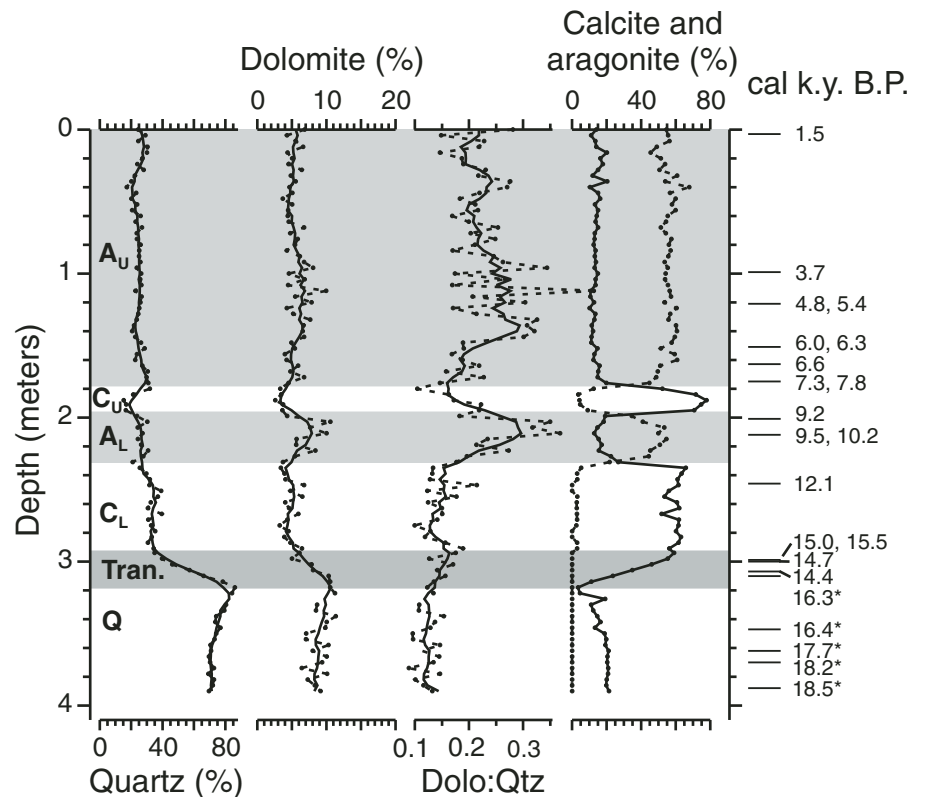


Figure 6. Mineralogic abundances and ratio of dolomite to quartz (Dolo:Qtz) for core BL96-1. The entire core is in the upper aragonite interval. For quartz, dolomite, and Dolo:Qtz, solid curves are drawn through five-point running means. Calcite content is shown by solid line and aragonite content is shown by dashed line. Calibrated ^{14}C ages are from Colman et al. (this volume).

Figure 7. Mineralogic abundances and ratio of dolomite to quartz (Dolo:Qtz) for core BL96-2. The upper aragonite (A_U), upper calcite (C_U), lower aragonite (A_L), and lower calcite (C_L) intervals make up the carbonate-rich upper unit. A transition zone (Tran.) lies between the upper unit and the quartz-rich lower unit (Q). For quartz, dolomite, and Dolo:Qtz, solid curves are drawn through five-point running means. Calcite content is shown by solid line and aragonite content is shown by dashed line. Calibrated ^{14}C ages (asterisk indicates age from correlation to core BL00-1) are from Colman et al. (this volume).



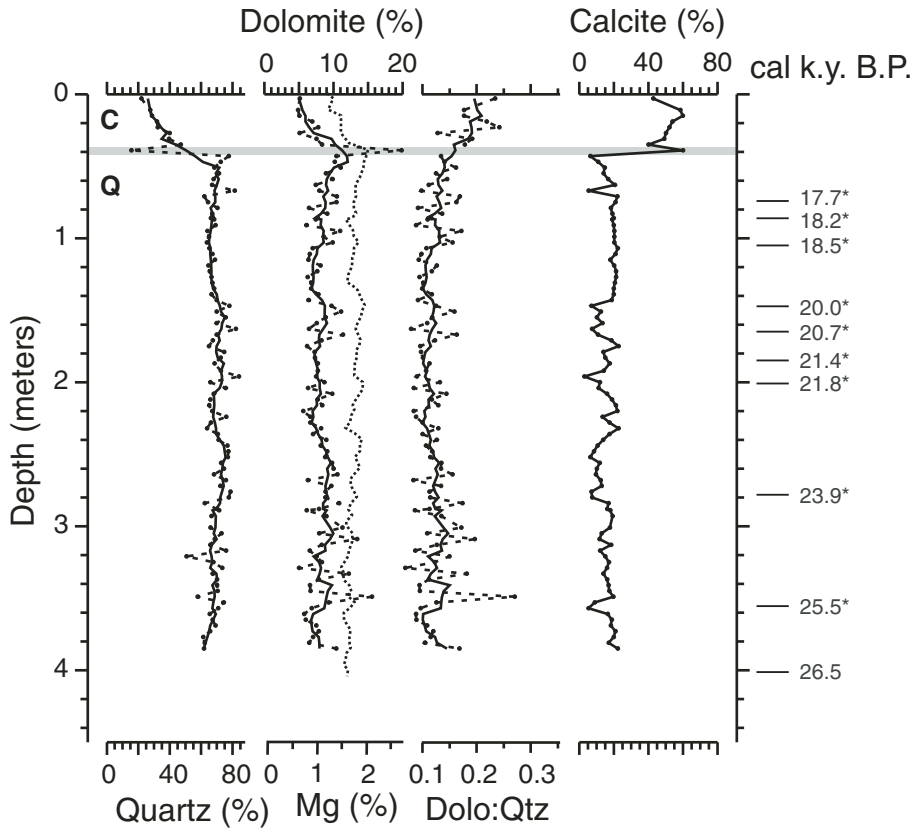
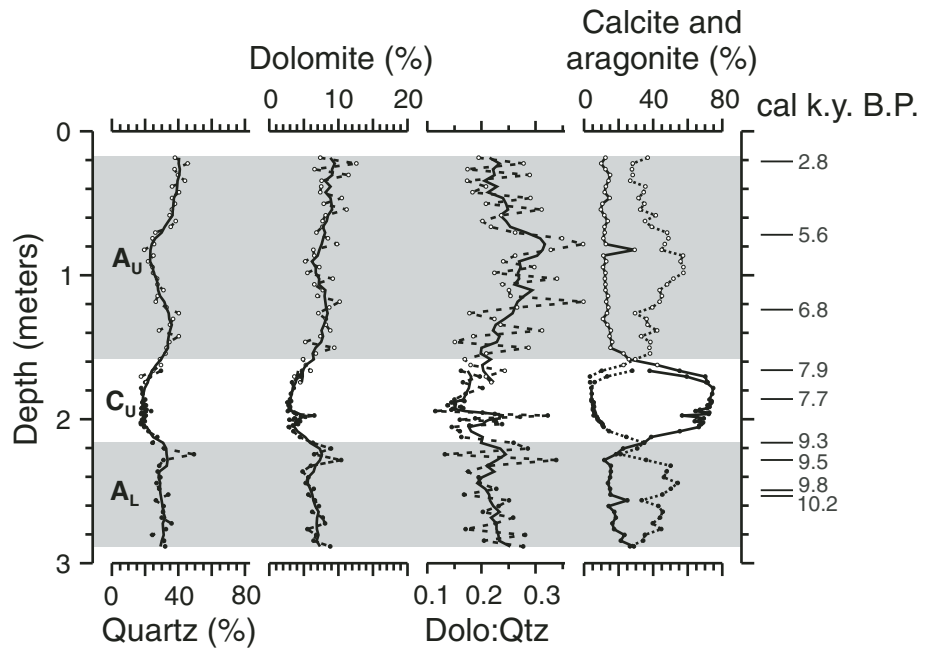


Figure 8. Mineralogic abundances, content of Mg (dotted line), and ratio of dolomite to quartz (Dolo:Qtz) for core BL96-3. The carbonate-rich upper unit (C) and transition zone (horizontal gray band) are thin, relative to other cores. For quartz, dolomite, and Dolo:Qtz, solid curves are drawn through five-point running means. Calibrated ^{14}C ages (asterisk indicates age from correlation to core BL00-1) are from Colman et al. (this volume).

Figure 9. Mineralogic abundances and ratio of dolomite to quartz (Dolo:Qtz) for core BL2002-3. The core penetrated the upper aragonite (A_U), upper calcite (C_U), and lower aragonite (A_L) intervals. Open and closed symbols indicate data from two overlapping core segments. For quartz, dolomite, and Dolo:Qtz, solid curves are drawn through five-point running means. Calcite content is shown by solid line and aragonite content is shown by dashed line. Calibrated ^{14}C ages are from Colman et al. (this volume).



Elemental Chemistry

Variations in contents of Al, Ti, Mg, and Ca within core BL96-3 (Fig. 11) reflect changes in mineralogy like those described above, but because of the high precision of the chemical data some variations are evident in these elements that are not clearly observed in the mineralogy. The chemically immobile elements Al and Ti provide convenient proxies for the non-carbonate detrital material and, like quartz (Fig. 8), they decline upward from the lower unit into the upper unit (Fig. 11). Similarly, across the unit boundary Mg and Ca mimic the upward decrease in dolomite and increase in calcite (Fig. 8), respectively.

In addition to the major changes across the unit boundaries described above, small variations in the contents of Al, Ti, and Mg are evident within the lower unit. These changes are most evident in plots of Mg and of elemental ratios (Fig. 11). Mg from the HCl-soluble carbonate minerals (Bischoff et al., 2005) closely matches the magnitude and variations expected from variations in dolomite. Values of Mg:Ca and Mg:Al have very similar variations throughout the lower unit and diverge abruptly at the unit boundary as Ca content begins to increase due to the precipitation of endogenic calcite. Inspection of Figure 11 reveals that relative maxima and minima in Ti:Al, Mg:Ca, and Mg:Al coincide.

The content of sulfur is uniformly low throughout most of the lower unit, but begins to increase ~30 cm below the transition to the upper unit and peaks at the unit boundary (Fig. 11). Sulfur generally decreases upward through the truncated upper unit sampled at this locality, but remains much higher than throughout most of the lower unit.

Magnetic Properties

Within the quartz-rich lower unit, between the bottom of core BL96-3 and a depth of 1.05 m, magnetic properties vary in a quasi-cyclical manner (Fig. 12). Properties indicative of magnetite content both in an absolute sense (MS, ARM, and IRM) and relative to hematite (S) are strongly correlated. In this interval, there is a negative relation between these properties and HIRM, which indicates hematite content. This part of the lower unit yields nearly identical results in a 120-m-thick cored section (BL00-1, Fig. 2) studied by Heil et al. (this volume). MS features labeled 9–14 and HIRM features labeled 1–10 (Fig. 12) can be unequivocally identified in both records and were used in correlating the two sections and transferring ^{14}C ages to the long core (Colman et al., 2006; Colman et al., this volume).

The relation between the contents of magnetite and hematite changes in the upper part of the lower unit. On the basis of

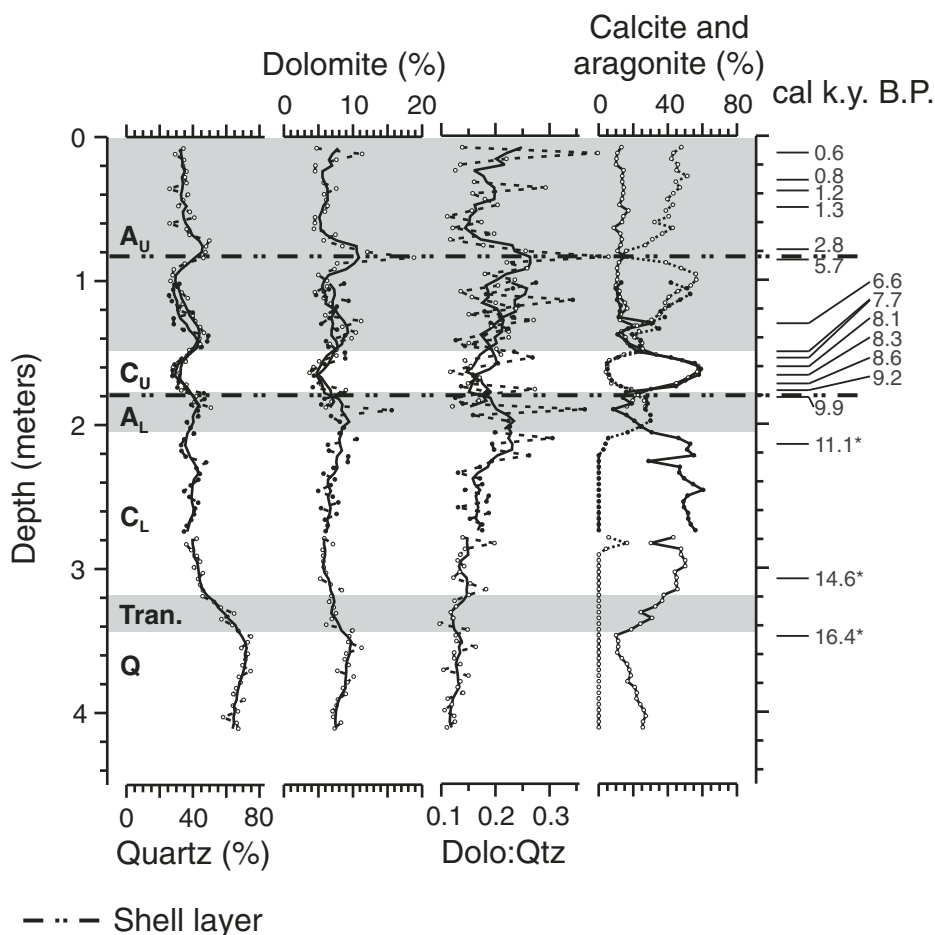


Figure 10. Mineralogic abundances and ratio of dolomite to quartz (Dolo:Qtz) for core BL2002-4. The upper aragonite (A_u), upper calcite (C_u), lower aragonite (A_L), and lower calcite (C_L) intervals make up the carbonate-rich upper unit. A transition zone (Tran.) lies between the upper unit and the quartz-rich lower unit (Q). Open and closed symbols indicate data from three core segments. For quartz, dolomite, and Dolo:Qtz, solid curves are drawn through five-point running means. Calcite content is shown by solid line and aragonite content is shown by dashed line. Calibrated ^{14}C ages (asterisk indicates age from correlation to core BL00-1) are from Colman et al. (this volume).

TABLE 3. MASS ACCUMULATION RATES FOR CARBONATE-RICH UPPER UNIT AND QUARTZ-RICH LOWER UNIT

Core	Water depth (m)	Depth to top of interval (cm)	Depth to bottom of interval (cm)	Age at top of interval (cal. yr B.P.)	Age at bottom of interval (cal. yr B.P.)	Average density (g cm ⁻³)	Average carbonate mineral content (%)			Total MAR (g m ⁻² yr ⁻¹)	Carbonate mineral MAR (g m ⁻² yr ⁻¹)		Non-carbonate mineral MAR (g m ⁻² yr ⁻¹)
							Average carbonate mineral content (%)	Average quartz content (%)	Average non-carbonate mineral content (%)		Carbonate mineral MAR	Quartz MAR	
Carbonate-rich upper unit													
BL2002-4	34.9	8	76	110	2500	0.392	60.0	35.7	40.0	107	64	38	43
		80	176	5460	8850	0.759	58.1	36.2	41.9	215	125	78	90
		180	315	9060	15,150	0.746	56.8	38.5	43.2	168	95	64	73
					Weighted average	0.693	57.6	37.5	42.4	169	103	63	72
Quartz-rich lower unit													
BL2002-3	42.9	18.5	288.5	2740	11,520	0.794	67.4	27.8	32.6	238	160	66	78
BL96-2	43.0	0	294	1310	14,520	0.724	72.8	26.3	27.2	161	117	42	44
BL96-1	50.0	2	498	650	7710	0.808	78.1	21.9	21.9	567	442	124	124
Quartz-rich lower unit													
BL96-3	33.0	43	385	16,680	25,920	1.090	24.0	69.4	76.0	403	96	280	306
BL2002-4	34.9	345	413	16,570	19,860	1.038	27.4	68.5	72.6	215	59	147	156
BL96-2	43.0	320	396	15,730	18,980	0.971	25.4	74.5	74.0	227	58	169	169

Note: For BL2002-4, mass accumulation rates (MAR) were calculated for intervals between prominent unconformities marked by shell layers and as a weighted average for the three intervals. Mineral content was determined by X-ray diffraction. Carbonate-mineral content is the sum of calcite, aragonite, and dolomite contents. Ages based on age-depth models described in Colman et al. (this volume).

the locations of the transition from the lower to the upper unit, the shape of the HIRM curve, and comparable values of HIRM, the maximum value of HIRM in BL96-3 ($9.5 \times 10^{-4} \text{ Am}^2 \text{ kg}^{-1}$) at 1.05 m (Fig. 12) correlates with the HIRM peak in BL96-2 ($8.6 \times 10^{-4} \text{ Am}^2 \text{ kg}^{-1}$) at 3.88 m (Fig. 13), and a secondary peak in BL96-3 ($6.4 \times 10^{-4} \text{ Am}^2 \text{ kg}^{-1}$) at 0.76 m correlates with a peak in BL96-2 ($5.9 \times 10^{-4} \text{ Am}^2 \text{ kg}^{-1}$) at 3.62 m. Between these peaks, changes in HIRM are not matched by changes in MS comparable to those that accompany variations in HIRM below 1.05 m in BL96-3. In both BL96-2 and -3, HIRM decreases upward from the secondary peak to the top of the lower unit. However, the magnitude of this decrease differs in the two cores, with HIRM decreasing by factors of 5.1 and 1.7 in BL96-3 and -2, respectively. MS curves in this interval differ markedly. MS values in BL96-3 decrease gradually to the upper boundary of the lower unit, whereas values in BL96-2 increase gradually immediately above the secondary HIRM peak and then more abruptly from 3.32 m to the boundary. This change in rate of increase in MS is also present in the record from BL2002-4 (Fig. 14).

Both MS and HIRM generally decrease upward across the transition between the lower and upper units and continue to decrease in the lower part of the upper unit. Two MS peaks (one labeled 6 in Figs. 13, 14, and 15, and the other labeled 7 in Figs. 13 and 14) interrupt the general decrease in MS. These peaks occur near the lower and upper boundaries of the lower calcite interval. Both MS and HIRM attain very low values in the lower aragonite interval. HIRM then remains low before increasing near the top of the section. The MS records contain several low-amplitude peaks overlying the lower aragonite interval (Figs. 14–16), but only the lowermost of these (labeled 5), which coincides with the upper calcite interval, and an (unnumbered) increase near the top of the section are recognized in more than one core. Individual peaks in MS (1–4), ARM, and IRM in core BL96-1 (Fig. 16) may correlate with zones of slightly elevated values in cores BL2002-3 (Fig. 15) and BL2002-4 (Fig. 14), but similar features do not occur in core BL96-2 (Fig. 13). Magnetic susceptibility peaks 5 and 6 coincide with intervals interpreted as periods of high lake level (Smoot and Rosenbaum, this volume), whereas peak 7 immediately overlies a similar high lake-level interval.

In the lower unit, which is characterized by magnetic properties indicative of relatively abundant magnetite and hematite, petrographic observations of magnetic separates show that detrital magnetic minerals commonly occur as fine-silt-sized (<10 μm), angular particles, or within rock fragments of similar size and shape (Reynolds and Rosenbaum, 2005). Magnetite is the most abundant mineral in eight of 12 magnetic separates (Figs. 12 and 13). Detrital hematite is the second most common mineral in most of the magnetite-rich separates, is subequal to magnetite in one separate, and is the most abundant mineral in three separates. Samples included in these four hematite-rich separates are all from peaks in HIRM. The magnetite occurs in many forms, including titaniferous magnetite, low-titanium magnetite, and as crystals within rock fragments. Hematite occurs mainly in reddened rock fragments and as particles

of specular hematite. The reddened rock fragments comprise many different lithic types, but siltstone is the most abundant type in the hematite-rich samples. Iron sulfide minerals are rare. Minor framboidal pyrite is present in two separates and small amounts of griegite are present in four separates at depths greater than 1 m in core BL96-3. The two uppermost separates from the lower unit in BL96-3, which sampled peaks in IRM/MS (Fig. 12), contain more plentiful griegite. There is no petrographic evidence for the dissolution of detrital magnetic grains from the lower unit.

Magnetite is also the most common mineral in the one separate from the transition zone between the lower and upper units in BL96-2 (Fig. 13). The magnetite, which occurs largely as optically homogeneous grains and in rock fragments, shows possible minor dissolution. This is the only magnetic separate studied that contains common pyrite framboids.

Magnetite is the most abundant mineral in five of eight separates from the upper unit (Reynolds and Rosenbaum, 2005). Magnetic properties indicate that this unit has generally low concentrations of both magnetite and hematite (Figs. 13 and 14). The magnetite occurs mostly as small grains and in rock fragments, and, in several separates, shows some evidence of dissolution. Several of the separates are notable. The separate from ~2.80 m in BL96-2, just above the transition zone,

contains relatively abundant material and is the only separate that contains large (~70 μm) grains of magnetite and large (~100 μm) rock fragments with magnetite inclusions. The separate that spans the MS peak at ~2.37 m contains a few magnetite-bearing volcanic glass shards in addition to magnetite as small grains and in rock fragments. The separate at a depth of 4.90 m in BL96-1, within a zone of very low MS (Fig. 16), is unique in that the most abundant mineral is titanohematite (referring to a range of compositions in the hematite-ilmenite solid solution series that are highly magnetic), although titanohematite is present in significant amounts in several other separates. Finally, no individual magnetite grains are present in the uppermost two separates from core BL96-1, which are located in a zone of very low MS. The only Fe-oxides in these separates occur within small rock fragments.

Grain Size

Surface samples from four depth transects (Fig. 2) were subjected to grain-size analyses. Each transect shows a decrease in grain size of the siliciclastic fraction with depth, but the relation between size and depth varies from profile to profile (Fig. 17). The northernmost transect, which has the most constant and lowest bottom slope (Fig. 2), is located close to core sites BL2002-3 and -4 and incorporates the uppermost samples from these cores.

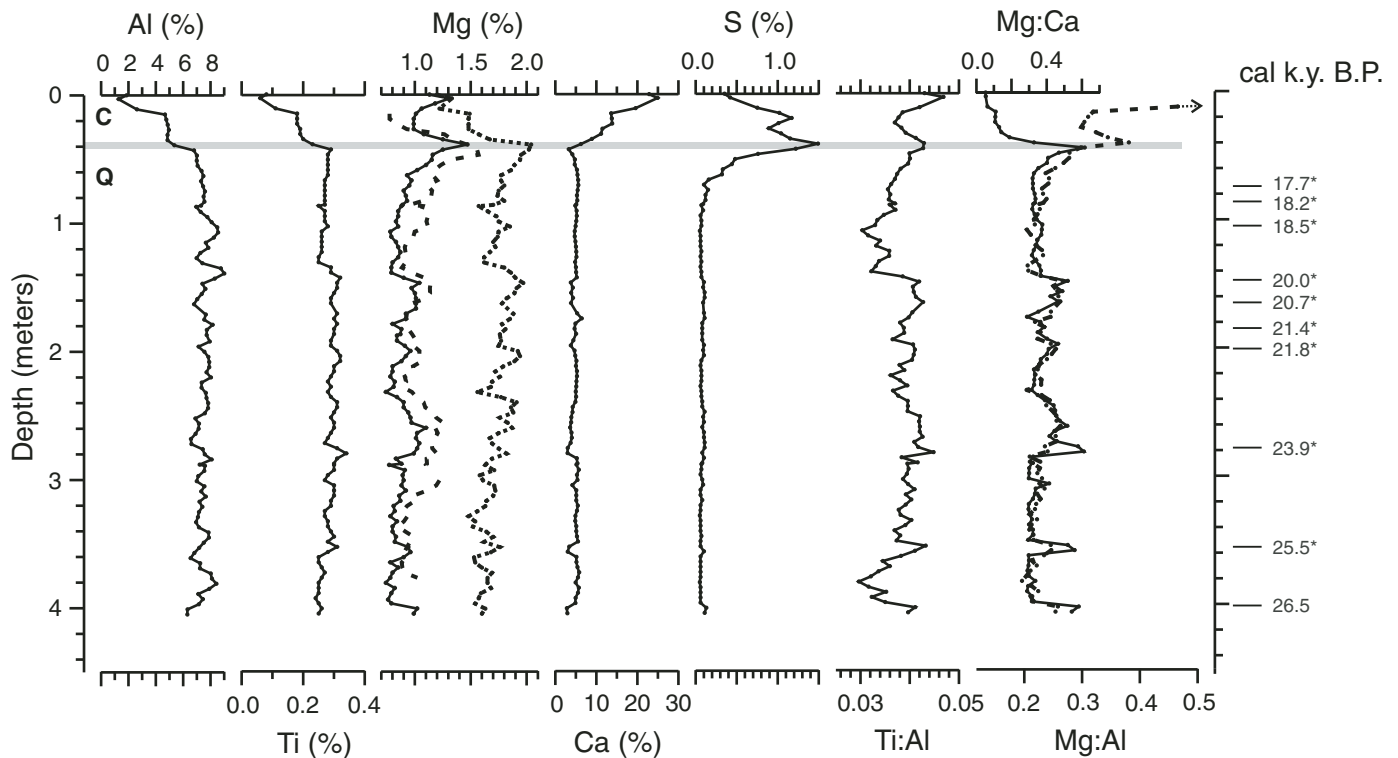


Figure 11. Abundances of selected elements and elemental ratios in core BL96-3. Calibrated ^{14}C ages (asterisk indicates age from correlation to core BL00-1) are from Colman et al. (this volume). Three curves are shown for Mg: (1) Mg from bulk samples (dotted), (2) HCl-extractable Mg (solid; Bischoff et al., 2005), and (3) Mg calculated from five-point running mean values of dolomite content (dashed) under the assumption of stoichiometric dolomite ($\text{CaMg}(\text{CO}_3)_2$). C and Q denote the carbonate-rich upper unit and quartz-rich lower unit, respectively.

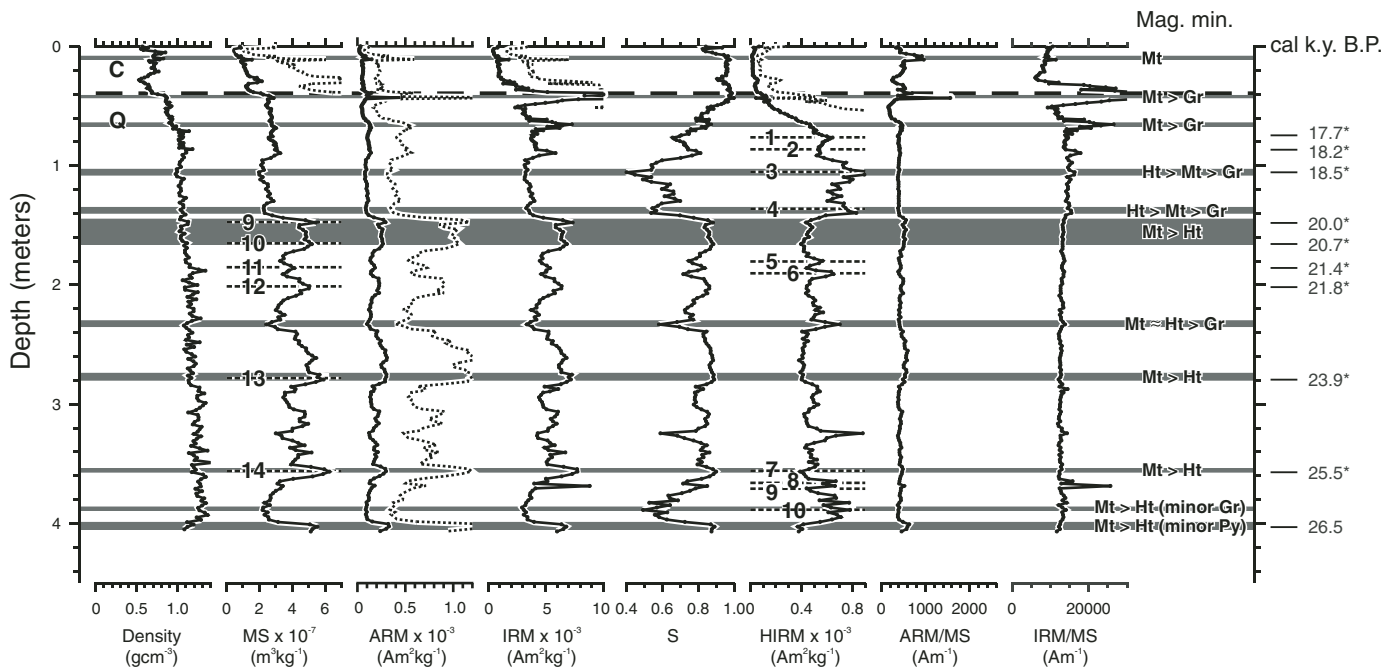


Figure 12. Density and magnetic properties for core BL96-3. In this figure, and in Figures 13–16, magnetic properties are magnetic susceptibility (MS), anhysteretic remanent magnetization (ARM), isothermal remanent magnetization (IRM), the S parameter, hard isothermal remanent magnetization (HIRM), and ratios ARM/MS and IRM/MS. Stratigraphic units (A_U —upper aragonite; C_U —upper calcite; A_L —lower aragonite; C_L —lower calcite intervals of the carbonate-rich upper unit, C; Tran.—the transition zone between the upper unit and the quartz-rich lower unit, Q) are delineated by alternating light-gray and white areas or by horizontal dashed lines. For comparison of low-amplitude features among cores, dotted curves are expanded by a factor of 4. Numbered features on the MS and HIRM plots are interpreted to correlate with features of the same numbers on plots of data from other cores. Relative amounts of magnetic minerals (Mag. min.) observed petrographically (Mt—magnetite; Ht—hematite; Ti-ht—titanohematite; Gr—greigite; Py—pyrite) are indicated on horizontal dark-gray bands, which indicate depth intervals sampled for magnetic separates. Calibrated ^{14}C ages (asterisk indicates age from correlation to core BL00-1) are from Colman et al. (this volume).

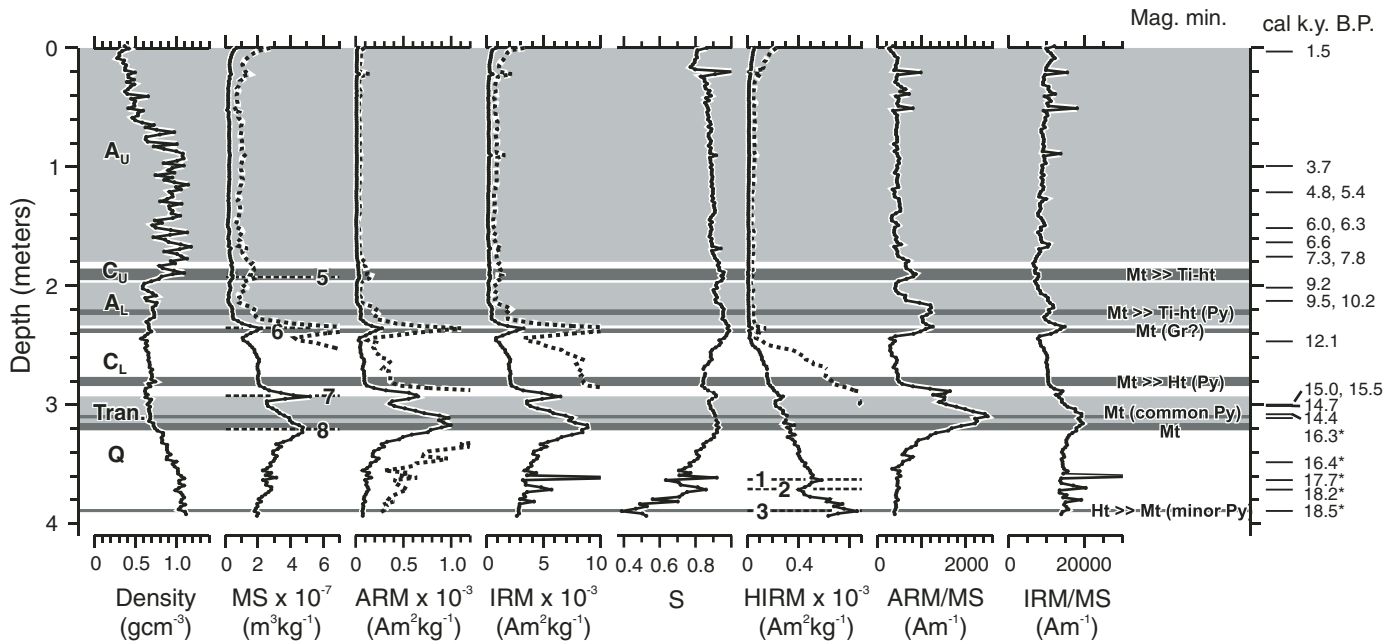


Figure 13. Density and magnetic properties for core BL96-2. See caption to Figure 12 for explanation.

This transect contains median grain sizes ranging from ~6 to 250 μm and yields a simple size-depth relation that is closer to that predicted by a wave model than those for the other transects (Smoot and Rosenbaum, this volume).

In the cored sediment, siliciclastic material from the lower unit is finer grained than that in the upper unit (Fig. 18). Median grain sizes in the lower unit range from <1 μm to 12 μm and aver-

age ~3 μm . Sand content averages less than 1%. Below ~0.55 m in core BL96-3, there appear to be well-defined fluctuations in grain size, even though the grain-size range is extremely narrow, with few samples having median grain sizes greater than 4 μm . The coarsest sediment in the lower unit occurs just below the transition to the upper unit. In the upper unit, median grain sizes range from ~3 to 39 μm and average ~15 μm . The average sand

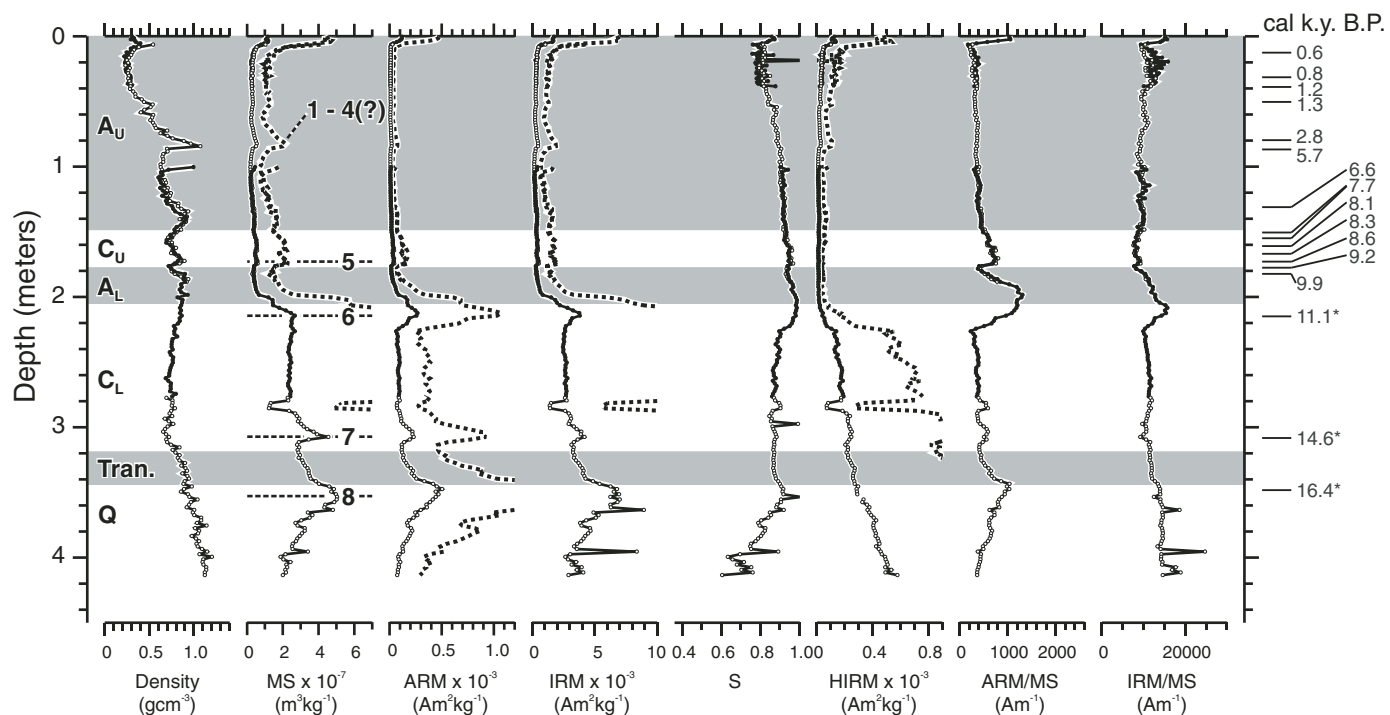


Figure 14. Density and magnetic properties for core BL2002-4. Open and closed symbols indicate data from three core segments. See caption to Figure 12 for explanation.

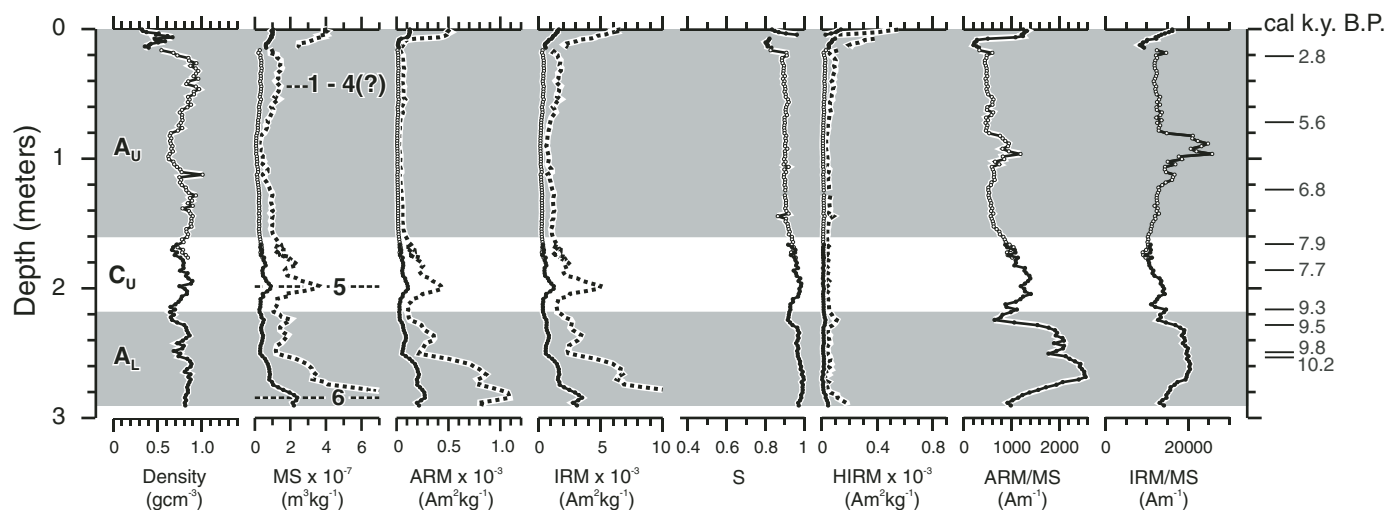


Figure 15. Density and magnetic properties for core BL2002-3. Open and closed symbols indicate data from two core segments. See caption to Figure 12 for explanation.

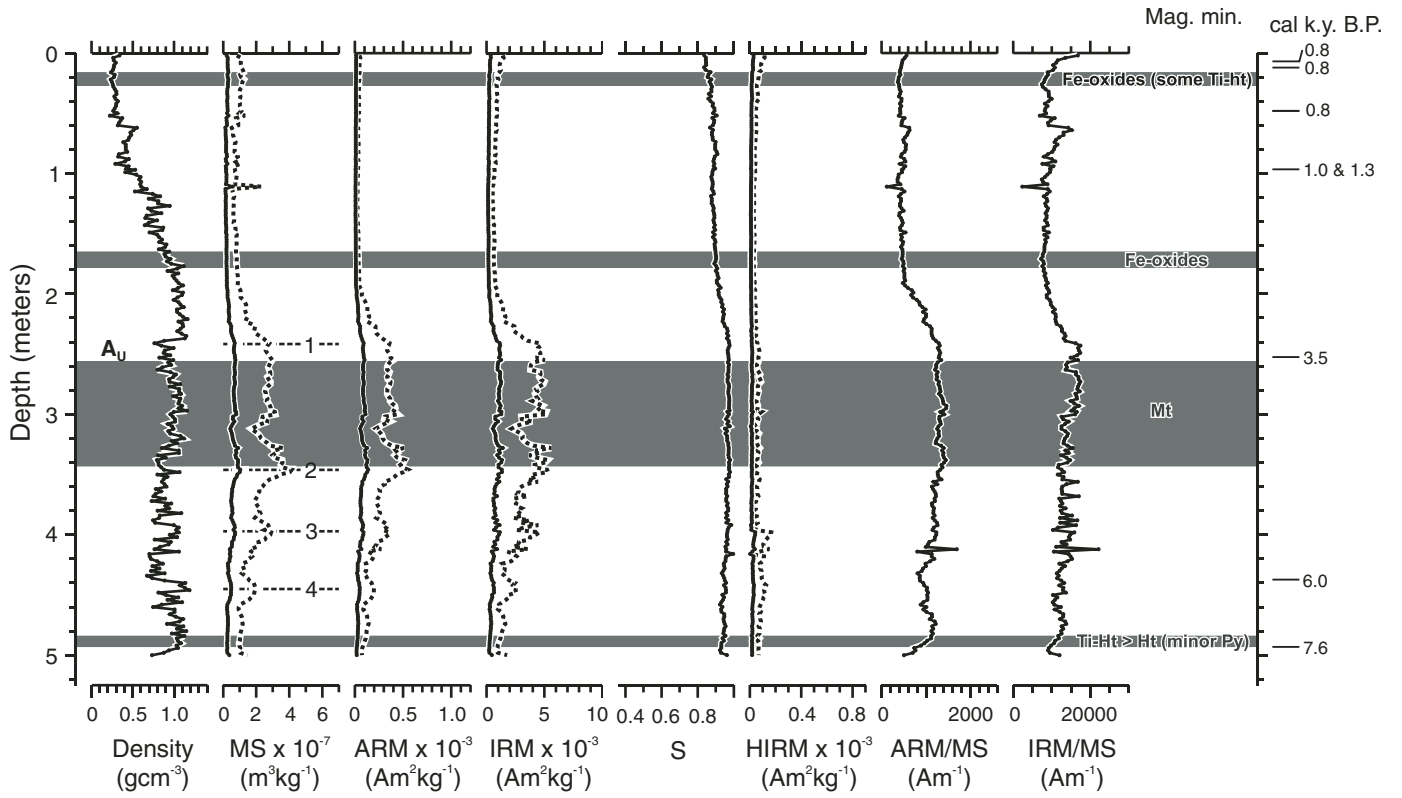


Figure 16. Density and magnetic properties for core BL96-1. See caption to Figure 12 for explanation.

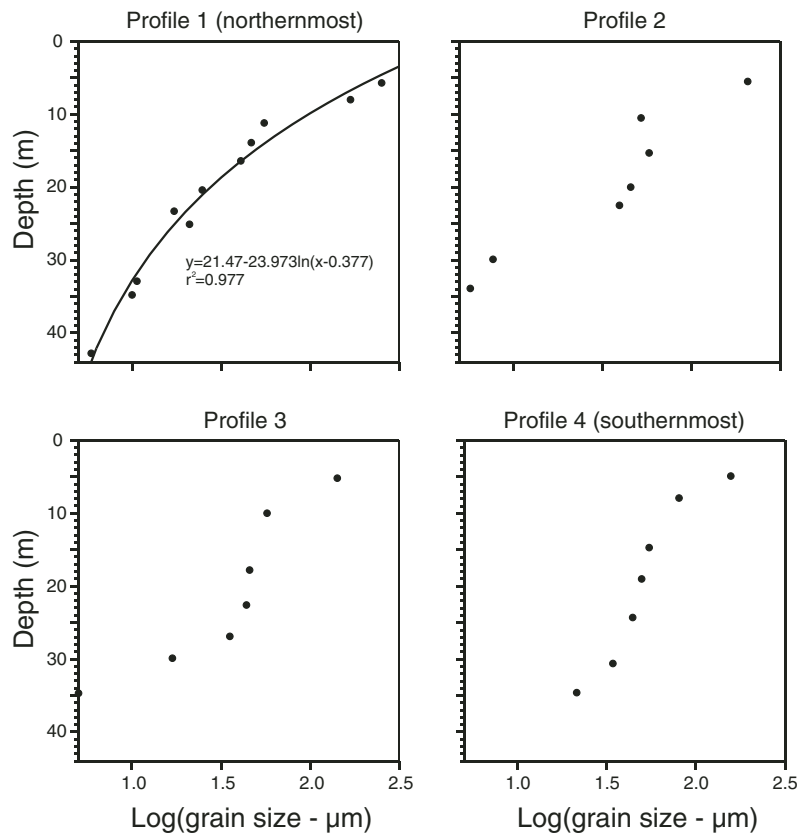


Figure 17. Median-grain-size data for surface samples versus water depth. Profile locations are in Figure 2. Equation and r^2 values are for curve fit to data from profile 1.

content of detrital material in the upper unit is ~9%. Well-defined variations in grain size of siliciclastic material correspond, at least in part, to changes in carbonate mineralogy. The lower calcite interval in BL2002-4 is relatively fine grained, with median grain size averaging 6 μm below 3.30 m and coarsening upward into the lower aragonite interval. Grain size is relatively coarse in the lower aragonite interval, decreases abruptly into the upper calcite interval, and then coarsens again into the upper aragonite interval. Most of the upper aragonite interval is relatively coarse grained, but grain size decreases in the upper 10–15 cm, becoming comparable to that in the lower part of the lower calcite interval. Two zones of coarse sediment in core BL2002-4 enclose shell layers at 0.84 and 1.80 m (Smoot, this volume), which are interpreted as beach or shallow-water deposits (Smoot and Rosenbaum, this volume). Stratigraphic position with respect to mineralogic zones and radiocarbon ages indicate that the lower of these coarse zones in BL2002-4 correlates with a zone from 2.10 to 2.35 m in BL2002-3 that contains two peaks in median grain size.

DISCUSSION

Fluvial Sediment Sources

Data from fluvial sediments indicate significant differences among four potential source areas of detrital sediment in Bear Lake (Table 1): (1) the west side of the local catchment (sites 1–12, Fig. 2), (2) the east side of the local catchment (sites 13–18), (3) the lower Bear River (sites 19–46), and (4) the upper Bear River (sites 47–54). These differences provide the means for interpreting changes in provenance within the cored lake sediment. Some of the differences reflect bedrock geology. Stream sediments from the east and west sides of the local Bear Lake catchment contain less quartz than sediment from the Bear River, reflecting abundant carbonate rocks in the Bear River Range and Bear Lake Plateau. These local catchment areas are differentiated by the abundance of carbonate minerals, with the west side sediments containing more dolomite and having high concentrations of Mg, and the east side sediments containing more calcite. The

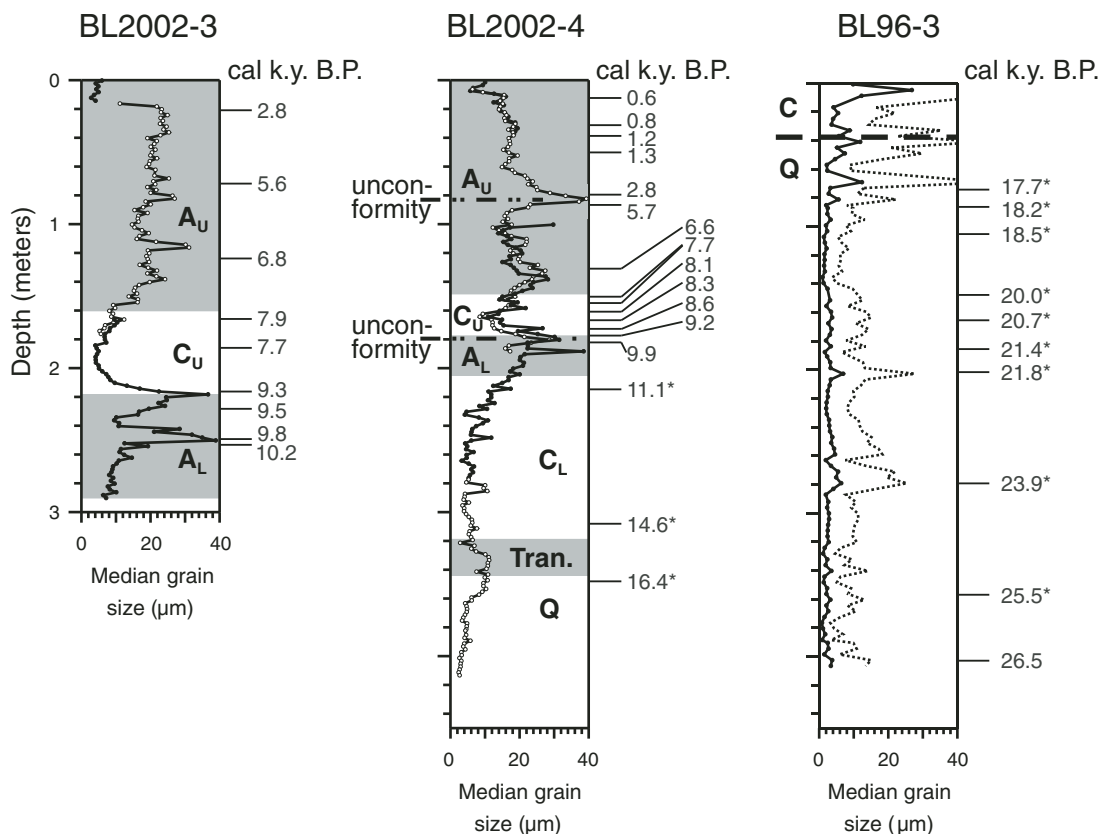


Figure 18. Median grain size versus depth for cores BL2002-3, BL2002-4, and BL96-3. For cores BL2002-3 and -4, open and closed symbols indicate individual core segments. Alternating gray and white zones and horizontal dashed line delineate the upper aragonite (A_U), upper calcite (C_U), lower aragonite (A_L), and lower calcite (C_L) intervals of the carbonate-rich upper unit (C), and the transition zone (Tran.) between the upper unit and the quartz-rich lower unit (Q). Calibrated ^{14}C ages (asterisk indicates age from correlation to core BL00-1) are from Colman et al. (this volume).

Bear River drains areas of widespread clastic sedimentary and metasedimentary rocks. As a result, its sediments contain more quartz and Al, and less Ca than sediments from the local catchment. Hematite content, as indicated by HIRM, is about twice as great in samples from the upper Bear River as in those from either the lower Bear River or the local catchment (Table 1, Fig. 5). The high hematite content in the upper Bear River is probably due to detritus derived from hematite-rich rocks of the Uinta Mountain Group (Ashby et al., 2005). High hematite content in the silt-and-clay fraction corresponds more closely to the extent of till of the last glaciation (Laabs et al., 2007) than to outcrops of the Uinta Mountain Group. Only sites 51–54 are located on Uinta Mountain Group bedrock (Fig. 1), and the maximum extent of last-glacial-aged till, which contains abundant detritus from Uinta Mountain Group rocks, lies between sites 45 and 47. In general, the content of Uinta Mountain Group detritus is diluted within a short distance downstream from the last-glacial limit, although, enhanced hematite content occurs sporadically in coarser fractions somewhat farther downstream, perhaps in outwash from which the fine-grained material has been winnowed.

In contrast to most of the mineralogical and geochemical data, the content of ferrimagnetic minerals, as measured by MS, is not related to bedrock geology. Values of MS for samples from within the local catchment are several times greater than MS values from Bear River sediment, and values from areas of Paleozoic rocks on the west side of the lake are similar to values from areas of Mesozoic rocks on the east side of the lake. Petrographic observations indicate that the stream sediments contain a wide variety of magnetic Fe-Ti-oxide mineral grains, many of which were formed at high temperature in igneous or metamorphic rocks that are lacking in the local Bear Lake drainage basin as well as that of the Bear River. Because the catchment rocks lack sources for many of the Fe-Ti-oxide grains, these grains are interpreted to have been introduced as atmospheric dust (Reynolds and Rosenbaum, 2005). The size of the magnetic grains, mostly <10 μm , is consistent with dust particles that can be transported hundreds of kilometers (Rose et al., 1998; Goudie and Middleton, 2006). These results suggest that the concentration of dust in streams in the local catchment is several times greater than in the sediments of the Bear River. The difference in dust concentration between sediments of the local catchment streams and those of the Bear River could reflect either a difference in the rate of dust deposition or a difference in the amount of dilution of dust by rock material derived from the catchment. Nevertheless, the large contrast in MS provides a potential tool to discriminate between detritus in the lake sediments that was derived from local streams and that derived from the Bear River.

Provenance of Detrital Material

Detrital materials incorporated in the lake sediments include (1) rock material derived through erosion of rocks within the drainage basin and delivered via fluvial transport; (2) dust deposited indirectly via fluvial transport following deposition in the

drainage basin; and (3) dust deposited directly in the lake. The limited data (two years) from three dust-trap locations on the north, east, and west sides of Bear Lake indicate relatively low rates of dust deposition (Table 2) compared to dust-fall rates in southwestern deserts (Reheis, 2006). It is not known how well the dust data represent either long-term modern dust deposition or rates of deposition prior to European settlement. Modern dust flux may have been enhanced by anthropogenic sources due to construction and agriculture in the region and even to recreational activities on local beaches. The dust fluxes are also low relative to mass accumulation rates of both carbonate and non-carbonate minerals in the lake sediments (Table 3). In the quartz-rich lower unit, accumulation rates of carbonate and non-carbonate minerals are respectively one and two orders of magnitude higher than in the dust samples. Because of reworking of sediment, especially during periods of low lake level (Smoot and Rosenbaum, this volume), little of the carbonate-rich upper unit exists in water shallower than ~30 m (Colman, 2006; Dean, this volume; Smoot, this volume). Approximately half the area of the full lake is above a depth of 30 m, so sediment focusing may have more or less doubled average mass accumulation rates below this depth. Even assuming a doubling of the observed rate of dust deposition in this unit, accumulation of endogenic carbonate is so rapid that dust contributes little to overall carbonate content of the sediment. Relative to carbonate minerals, fluxes of non-carbonate minerals are lower in the sediment and much higher in dust, so that direct dust deposition in the lake could account for roughly 10%–20% of the non-carbonate minerals in the upper unit.

Variations in mineralogy, elemental concentrations, and magnetic properties with depth in sediment cores may provide information about the source areas of detrital material. In the absence of large amounts of endogenic material, interpretation of mineral and elemental concentrations is straightforward. When detrital material is diluted by abundant endogenic material, such as in the upper unit, interpretations are more complex and more ambiguous. Similarly, magnetic properties provide a powerful tool to discriminate among source areas if post-depositional alteration has not destroyed detrital Fe-oxides or formed secondary magnetic phases.

Similarity between the contents of quartz (70%) and calcite (10%–20%) in the lower unit and the contents of these minerals in the fine-grained fraction of Bear River sediment (Fig. 3) suggests that the lower unit contains little, if any, endogenic calcite. In addition, several observations indicate that magnetic properties in most of the lower unit have been largely unaffected by post-depositional alteration. First, MS values (mostly $0.2\text{--}0.5 \times 10^{-6} \text{ m}^3 \text{ kg}^{-1}$) and HIRM values (mostly $0.3\text{--}0.8 \times 10^{-3} \text{ Am}^2 \text{ kg}^{-1}$) in the lower unit are large in comparison to the upper unit and comparable to values in the fluvial sediments (Fig. 5). Second, post-depositional destruction of Fe-oxides in a reducing environment should affect both magnetite and hematite and, therefore, cannot explain the negative correlation between indicators of magnetite content (i.e., MS, ARM, and IRM) and HIRM. And third, petrographic observations show no evidence of Fe-oxide dissolution

and indicate that sulfides are present only in trace amounts except in the uppermost part of the unit in core BL96-3, where magnetic separates contain significant amounts of greigite. Magnetic separates that contain significant amounts of greigite (at 41 and 65 cm in BL96-3, Fig. 12) fall within a zone of elevated sulfur (Fig. 11) and were selected to sample sediment that yielded high values of IRM/MS (Fig. 12), which has been shown to be a good indicator for the presence of this mineral (Reynolds et al., 1994, 1998). Within the sulfur-rich zone in BL96-3, both magnetite and hematite contents decrease upward to the top of the lower unit. In the correlative portion of BL96-2, hematite content decreases, but by a much smaller amount than in BL96-3, and magnetite content increases. Only a few samples near the base of core BL96-2 yield high values of IRM/MS (Fig. 13), suggesting that they contain some greigite. These observations indicate that magnetic minerals in the uppermost 25 cm of the lower unit in BL96-3 have undergone significant post-depositional alteration, and that magnetic minerals in the correlative part of BL96-2 have undergone no alteration or have been altered to a lesser extent.

Interpretation of changes in provenance is relatively straightforward below ~1.4 m in BL96-3 because there is little endogenic material, magnetic properties reflect unaltered detrital minerals, and there are obvious relations among various proxies. The observed variations in HIRM, MS, and dolomite content respectively reflect changes in the proportions of detrital material derived from three sources: Uinta Mountain Group rocks in the headwaters of the Bear River, dust, and bedrock in the Bear River Range. However, determining which source drives the changes is more problematic. One alternative is that variable rates of direct dust input dilute fluvial materials to different extents. Several observations make this alternative unlikely. Given the mass accumulation rates of modern dust and of lower unit sediments (Tables 2 and 3), it seems unlikely that direct dust input to the lake could have been high enough to strongly affect the concentrations of fluvial detritus. Furthermore, dilution of fluvial material by direct deposition of dust cannot explain the positive correlation between MS and dolomite content. Finally, zones with the highest acid-leachable Mg concentrations, 1.45–1.65 m and 2.60–2.80 m (Fig. 19), have concentrations of ~1%. This value is equivalent to ~13% dolomite, indicating that the sediments in these zones comprise largely material from the local catchment (Table 1). MS values in these zones (average $\sim 5 \times 10^{-7} \text{ m}^3 \text{ kg}^{-1}$) are also similar to values of the local catchment samples. It would be highly coincidental for direct dust deposition to the lake and independent fluvial deposition of dolomite to yield values so similar to those observed in modern stream sediments. Therefore, high MS values are interpreted to indicate high concentrations of dust reworked from the land surface. Variations in MS and dolomite are linked because dust and bedrock were delivered to the lake via streams. The negative relations between HIRM and dolomite content (as measured by HCl-extractable Mg) and between HIRM and MS in this part of the section (Fig. 19) are interpreted to arise from millennial-scale variations in the contents of Uinta Mountain Group-rich material delivered by the Bear River and of material from bedrock

and surface of the local catchment, with an increase in one causing dilution of the other. Grain size of siliciclastic material also varies in this part of the section, with finer grain size corresponding to higher content of Uinta Mountain Group material. The variations in content of Uinta Mountain Group material have been interpreted to reflect changes in concentrations of fine-grained glacial flour from the headwaters of the Bear River (Dean et al., 2006; Rosenbaum and Heil, this volume).

Variations in content of glacial flour could have arisen in a variety of ways, including changes in the stream flow within the local catchment, changes in the course of the Bear River that affected the location of its delta or at times allowed the river to bypass the lake, and changes in the flux of glacial flour driven by changes in the extent of glaciation. It is more likely that changes in lake sediment composition were driven by changes in the amount of material delivered by the relatively large sediment-laden Bear River than by changes in the amount of material delivered by the small streams in the local catchment. The nearly identical variations in magnetic properties in cores BL96-3 and BL00-1 (Rosenbaum and Heil, this volume), which are separated by 4.5 km (Fig. 2), suggest that changes in the location of the river and its delta were insignificant, because such changes would be expected to change the distribution of Bear River sediment within the lake. Because Bear Lake appears to produce endogenic carbonate minerals in the absence of the Bear River (Dean et al., 2006; Kaufman et al., this volume), the low, relatively constant content of calcite within the quartz-rich lower unit indicates that Bear River input was probably always present. We therefore favor an interpretation like that of Reynolds et al. (2004) and Rosenbaum and Reynolds (2004) for Upper Klamath Lake (Oregon), in which changes in the content of glacial flour were driven by changes in the extent of glaciers within the catchment.

The relations among proxies for Uinta Mountain Group material and for local catchment material change in the upper part of the lower unit. For descriptive purposes, the upper part of the lower unit has been divided into three zones (Fig. 19). In zone I the correlation between MS and dolomite content (HCl-extractable Mg) in the underlying sediment ceases, with dolomite content becoming high relative to MS. The lack of a close relation between MS and dolomite continues in zone II, and the strong negative relation between MS and HIRM ceases. An abrupt decrease in HIRM at the base of zone II is accompanied by a smaller than “expected” increase in MS, and the HIRM and MS curves diverge across the zone. Within this zone, HIRM generally decreases, whereas dolomite content generally increases. With the exception of one sample, median grain size remains small (mostly $\leq 5 \mu\text{m}$) from the base of the lower unit to the top of zone II. The zone II-III boundary was picked at a point of upward increases in dolomite and grain size in core BL96-3 and at similar increases in MS and dolomite in core BL96-2. (The absence of a similar increase in MS in BL96-3 is attributed to alteration, discussed above.)

In terms of provenance, these observations indicate the following sequence. First (zone I), content of dolomitic bedrock from

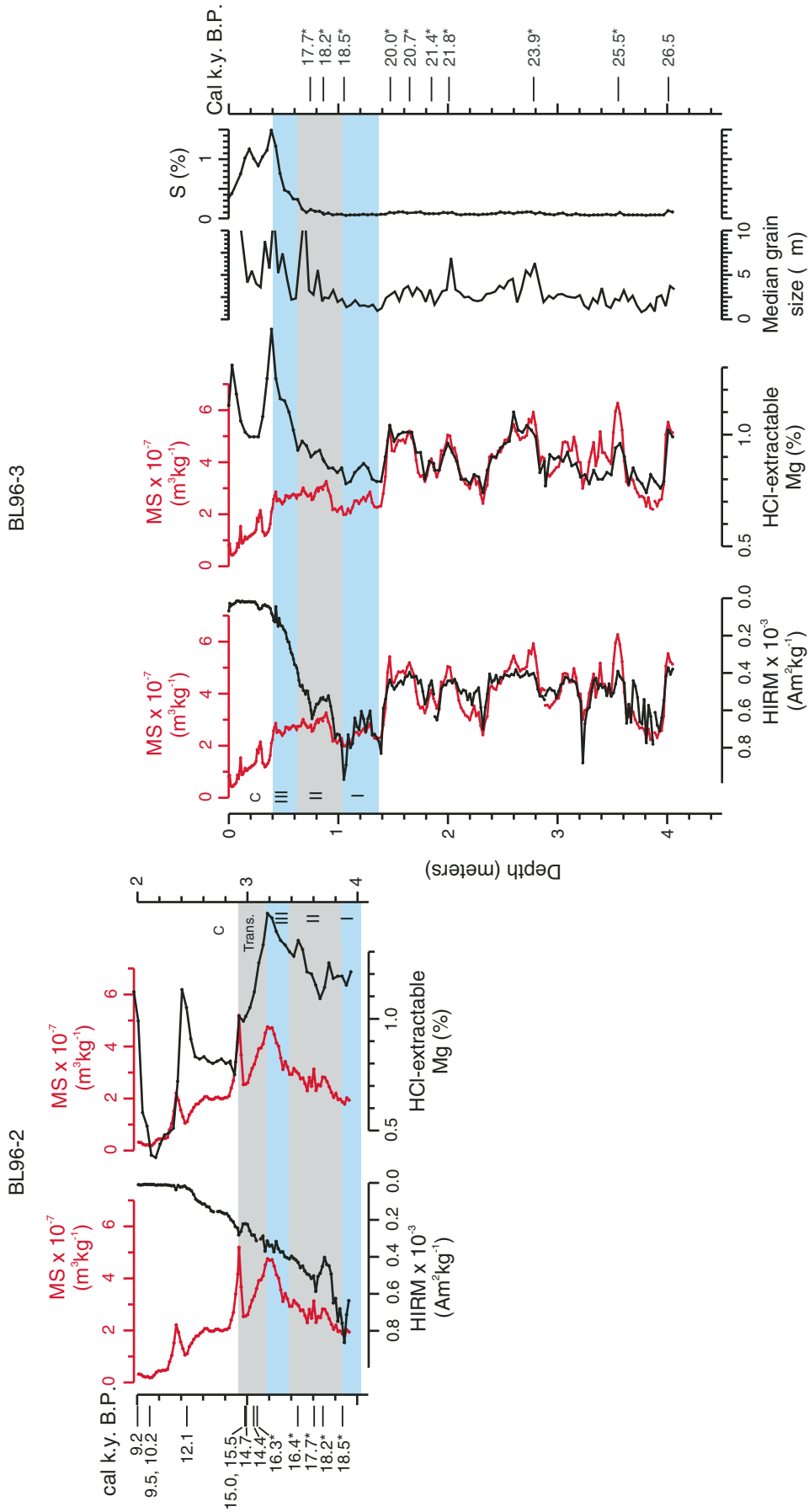


Figure 19. Comparison of magnetic susceptibility (MS), hard isothermal remanent magnetization (HIRM), and content of HCl-extractable Mg (Bischoff et al., 2005) in cores BL96-2 and -3, and median grain size and sulfur content in core BL96-3. Note inverted axis for HIRM. Below 1.2 m, MS is inversely related to HIRM ($MS = 7.905 \times 10^{-7} - 7.667 \times 10^{-4} \times HIRM$, $r^2 = 0.692$). Below 1.4 m, MS is positively correlated with HCl-extractable Mg ($MS = 8.602 \times 10^{-7} \times Mg - 3.529 \times 10^{-7}$, $r^2 = 0.681$). These relations were used to scale and position the MS curves with respect to HIRM and Mg. Zones I, II, and III at the top of the quartz-rich lower unit are defined for descriptive purposes (see text). The transition (Trans.) from the lower unit to the carbonate-rich upper unit (C) occurs abruptly at the top of zone III in core BL96-3 and more gradually in core BL96-2. Calibrated ¹⁴C ages (asterisk indicates age from correlation to core BL00-1) are from Colman et al. (this volume).

the Bear River Range increased while content of Uinta Mountain Group material remained high. The increase in dolomitic bedrock content was not accompanied by an increase in magnetite-bearing dust from the surface of the local catchment. Second (zone II), decreased content of hematite-rich Uinta Mountain Group material was accompanied by increased content of dolomitic material from the Bear River Range but with little corresponding change in surface material from the local catchment. Third (zone III), both magnetite-rich surface material and dolomitic bedrock from the local catchment increased, whereas the content of hematitic Uinta Mountain Group material declined. Rosenbaum and Heil (this volume) suggest that these variations in the upper portions of the lower unit may record (1) initial input of dolomitic glacial flour produced by growth of glaciers of Pinedale-equivalent age in the Bear River Range (Reheis et al., this volume) without a change in input of magnetite-rich surficial material; (2) growth of glaciers in the headwaters of the Bear River to extend down-valley beyond the extent of hematite-rich Uinta Mountain Group rocks onto less hematite-rich bedrock and concomitant growth of glaciers in the Bear River Range; and (3) decrease in glacial flour content due to glacial retreat or progressive abandonment of Bear Lake by the Bear River, or both.

As the Bear River largely abandoned Bear Lake, endogenic carbonate minerals increased and remained the dominant phases throughout the Holocene. However, the river's influence can be discerned within some intervals of the carbonate-rich upper unit. Dean et al. (2006) interpreted input of Bear River water during deposition of the upper and lower calcite intervals on the basis of geochemistry of the carbonate minerals. In addition, variations in detrital minerals suggest that Bear River sediment entered the lake during deposition of the calcite intervals. Specifically, Dolo:Qtz is generally lower within the calcite intervals than in the aragonite intervals (Figs. 7, 9, and 10) indicating that the local catchment detritus was diluted by quartz-rich, dolomite-poor Bear River sediment.

Above zone III, in the transition zone and the upper unit, magnetic properties as well as mineral and elemental concentrations are not useful indicators of changes in provenance. Low concentrations of Fe-oxide minerals reflect a combination of dilution by endogenic carbonate minerals and post-depositional destruction of detrital Fe-oxide minerals. Magnetic concentration parameters (e.g., MS, ARM, and HIRM) generally decrease upward across the lower calcite interval (Figs. 13 and 14) with little change in detrital material indicated by uniform quartz content (Figs. 7 and 10). This relation indicates a progressive upward increase in alteration of detrital Fe-oxide minerals and suggests an increase in salinity. This interpretation, that greater alteration of Fe-oxide minerals is associated with higher salinity, is consistent with the coincidence or near coincidence of peaks in magnetic concentration parameters (MS features 5–7 in Figs. 13–15) with interpreted high lake levels (Smoot and Rosenbaum, this volume), which presumably would coincide with reduced salinity. Variable Fe-oxide preservation and differences in detrital input probably contribute to low-amplitude variations in magnetic properties (MS features

1–4 in Figs. 14–16). For instance, higher values of MS within the upper aragonite interval in cores BL2002-3 and -4 (Figs. 15 and 14) generally coincide with slightly higher concentrations of detrital quartz (Figs. 9 and 10), whereas magnetic property variations in core BL96-1 (Fig. 16) are not accompanied by similar variations in quartz content (Fig. 6) and are therefore likely caused by differences in preservation of magnetic minerals.

Grain-Size Variations

The observed variation in grain size of modern sediment with water depth has little bearing on interpretation of grain-size variations in the quartz-rich lower unit because conditions during deposition of that unit were very different than at present. During that interval, the Bear River had glaciers in its headwaters and was connected to Bear Lake, the lake probably overflowed continuously, and sedimentation was dominated by fine-grained clastic material. These conditions are similar to those in glacial-aged sediment from Upper Klamath Lake (Oregon), where Reynolds et al. (2004) found variations in bulk sediment grain size, and interpreted finer grain size to reflect higher content of very fine grained glacial flour. Below 1.05 m in core BL96-3, variations in grain size probably reflect variations in glacial-flour content, with finer-grained sediments, which tend to have higher values of HIRM (Fig. 19), containing a higher proportion of glacial flour derived from hematite-rich Uinta Mountain Group rocks. The very fine grain size of less hematite-rich sediment between 1.05 and 0.6 m may also indicate a high content of glacial flour (Rosenbaum and Heil, this volume), but with less Uinta Mountain Group material (i.e., lower HIRM) and more dolomite than in sediments below 1.05 m.

During deposition of the carbonate-rich upper unit, conditions were much closer to those of the modern lake. Grain sizes are generally coarser than in the lower unit, and the coarsest sediment coincides with shell layers, which are interpreted to be beach or shallow-water deposits. The calcite intervals are generally finer grained than the aragonite intervals, suggesting deeper and shallower depositional environments, respectively. For the upper unit, the relation between grain size and water depth for the modern sediments can be used to estimate water depths in the past. Although the depth/grain-size relations differ among the surface profiles (Fig. 17), the location and consistent bottom slope of profile 1 (Fig. 2) make it the obvious choice for modeling paleodepths for cores BL2002-3 and -4. Smoot and Rosenbaum (this volume) combined this type of modeling with detailed sedimentology and paleo-shoreline data to create a lake-level curve.

SUMMARY

Study of modern fluvial sediment and dust provides insights into the origin of variations in the allogenic component of Bear Lake sediment. Two observations that reflect bedrock geology and help determine provenance of the lake sediment are (1) that dolomite content is high in streams draining the Bear River Range

on the west side of the lake, and (2) that HIRM values are high in the glaciated headwaters of the Bear River and probably reflect high content of hematite-rich detritus from Uinta Mountain Group rocks. Another observation that contributes to interpretation of provenance is provided by magnetic properties that measure the content of ferrimagnetic minerals (e.g., MS), which largely reflect silt-sized magnetite and titanomagnetite grains that were delivered to the catchment as a component of dust. The concentration of these magnetic grains is about three times higher in streams within the local Bear Lake catchment than in the Bear River.

The above observations are useful in interpreting the origin of mineralogical and magnetic property variations in the siliclastic lower unit penetrated by cores in Bear Lake because this unit contains little if any endogenic carbonate minerals and its magnetic properties are largely unaffected by post-depositional alteration. Within this unit, quasi-cyclical variations in grain size, HIRM, dolomite content, and MS generally reflect changes in content of very fine grained hematite-rich Uinta Mountain Group detritus delivered to the lake by the Bear River, and of somewhat coarser fluvial material from the local catchment that is rich in dolomite from the bedrock and in magnetite from dust on the land surface. Several factors contribute to an interpretation of the Uinta Mountain Group detritus as glacial flour. First, extensive glaciers were present in the headwaters of the Bear River during the last glacial period. Second, Uinta Mountain Group bedrock is exposed in a small fraction of the catchment. However, Uinta Mountain Group material is abundant in last-glacial-aged till but is largely absent in modern stream sediments downstream from the last glacial limit. Glaciers would have enhanced erosion and provided a source of fine-grained Uinta Mountain Group detritus to the Bear River. And last, below 1.05 m in core BL96-3, the tendency of sediment with a higher content of Uinta Mountain Group material to be finer grained is similar to the relation observed in Upper Klamath Lake (Oregon), where very fine grained, fresh basaltic detritus is interpreted to be glacial flour (Reynolds et al., 2004; Rosenbaum and Reynolds, 2004). In the upper part of the quartz-rich lower unit, the relations among grain size, HIRM, dolomite content, and MS differ from those observed below 1.4 m in core BL96-3. An increase in content of dolomitic bedrock from the local catchment without an increase in dust from the catchment surface or a change in Uinta Mountain Group material is followed by a decrease in Uinta Mountain Group detritus. Although the decrease in Uinta Mountain Group material was previously interpreted to reflect glacial retreat in the Uinta Mountains (Dean et al., 2006), the combined proxies may be more consistent with growth of Uinta glaciers beyond exposures of Uinta Mountain Group rocks and growth of glaciers in the Bear River Range (Rosenbaum and Heil, this volume).

Mineral and elemental concentrations and magnetic properties are less useful for determining provenance of detrital material in the upper unit because of the effects of dilution by large amounts of endogenic carbonate minerals and of post-depositional destruction of detrital Fe-oxide minerals. Nevertheless, relatively low values of Dolo:Qtz in the calcite-rich intervals indicate that

Bear River delivered sediment to the lake during deposition of these intervals. Within this unit, variations in grain size of siliclastic material largely reflect changes in water depth.

ACKNOWLEDGMENTS

We thank C. Chapman, J. Honke, G. Skipp, and F. Urban for assistance in coring, sampling, and laboratory analyses. L. Brown, H. Goldstein, T. Johnson, M. Rosen, and G. Skipp provided constructive reviews. This work was funded by the Earth Surface Dynamics Program of the U.S. Geological Survey.

ARCHIVED DATA

Archived data for this chapter can be obtained from the NOAA World Data Center for Paleoclimatology at <http://www.ncdc.noaa.gov/paleo/pubs/gsa2009bearlake/>.

REFERENCES CITED

- Ashby, J.M., Geissman, J.W., and Weil, A.B., 2005, Paleomagnetic and fault kinematic assessment of Laramide-age deformation in the eastern Uinta Mountains or, has the eastern end of the Uinta Mountains been bent? *in* Dehler, C.M., Pederson, J.L., Sprinkel, D.A., and Kowallis, B.J., eds., *Uinta Mountain geology: Salt Lake City, Utah Geological Association Publication 33*, p. 285–320.
- Bischoff, J.L., Cummins, K., and Shamp, D.G., 2005, Geochemistry of sediments in cores and sediment traps from Bear Lake, Utah and Idaho: U.S. Geological Survey Open-File Report 2005-1215, <http://pubs.usgs.gov/of/2005/1215/> (accessed June 2007).
- Bryant, B., 1992, Geologic and structure maps of the Salt Lake City 1° × 2° quadrangle, Utah, and Wyoming: U.S. Geological Survey Miscellaneous Investigations Series Map I-1997, scale 1:250,000.
- Colman, S.M., 2006, Acoustic stratigraphy of Bear Lake, Utah-Idaho—Late Quaternary sedimentation patterns in a simple half graben: *Sedimentary Geology*, v. 185, p. 113–125, doi: 10.1016/j.sedgeo.2005.11.022.
- Colman, S.M., Kaufman, D.S., Bright, J., Heil, C., King, J.W., Dean, W.E., Rosenbaum, J.G., Forester, R.M., Bischoff, J.L., Perkins, M., and McGeehin, J.P., 2006, Age models for a continuous 250-kyr Quaternary lacustrine record from Bear Lake, Utah-Idaho: *Quaternary Science Reviews*, v. 25, p. 2271–2282, doi: 10.1016/j.quascirev.2005.10.015.
- Colman, S.M., Rosenbaum, J.G., Kaufman, D., Dean, W.E., and McGeehin, J.P., 2009, this volume, Radiocarbon ages and age models for the last 30,000 years in Bear Lake, Utah-Idaho, *in* Rosenbaum, J.G., and Kaufman, D.S., eds., *Paleoenvironments of Bear Lake, Utah and Idaho, and its catchment: Geological Society of America Special Paper 450*, doi: 10.1130/2009.2450(05).
- Dean, W.E., 2009, this volume, Endogenic carbonate sedimentation in Bear Lake, Utah and Idaho, over the last two glacial-interglacial cycles, *in* Rosenbaum, J.G., and Kaufman, D.S., eds., *Paleoenvironments of Bear Lake, Utah and Idaho, and its catchment: Geological Society of America Special Paper 450*, doi: 10.1130/2009.2450(07).
- Dean, W.E., Rosenbaum, J.G., Skipp, G., Colman, S.M., Forester, R.M., Liu, A., Simmons, K., and Bischoff, J.L., 2006, Unusual Holocene and late Pleistocene carbonate sedimentation in Bear Lake, Utah and Idaho, USA: *Sedimentary Geology*, v. 185, p. 93–112, doi: 10.1016/j.sedgeo.2005.11.016.
- Dean, W.E., Wurtsbaugh, W., and Lamarra, V., 2009, this volume, Climatic and limnologic setting of Bear Lake, Utah and Idaho, *in* Rosenbaum, J.G., and Kaufman, D.S., eds., *Paleoenvironments of Bear Lake, Utah and Idaho, and its catchment: Geological Society of America Special Paper 450*, doi: 10.1130/2009.2450(01).
- Denny, J.F., and Colman, S.M., 2003, Geophysical Surveys of Bear Lake, Utah-Idaho, September 2002: U.S. Geological Survey Open-File Report 03-150.
- Dover, J.H., 1995, Geologic map of the Logan 30' × 60' quadrangle, Cache and Rich counties, Utah, and Lincoln and Uinta counties, Wyoming: U.S. Geological Survey Miscellaneous Investigations Series Map I-2210 scale, 1:100,000.

- Goudie, A.S., and Middleton, N.J., 2006, Desert dust in the global system: New York, Springer, 287 p.
- Heil, C.W., Jr., King, J.W., Rosenbaum, J.G., Reynolds, R.L., and Colman, S.M., 2009, this volume, Paleomagnetism and environmental magnetism of GLAD800 sediment cores, Bear Lake, Utah and Idaho, in Rosenbaum, J.G., and Kaufman, D.S., eds., Paleoenvironments of Bear Lake, Utah and Idaho, and its catchment: Geological Society of America Special Paper 450, doi: 10.1130/2009.2450(13).
- Kaufman, D.S., Bright, J., Dean, W.E., Moser, K., Rosenbaum, J.G., Anderson, R.S., Colman, S.M., Heil, C.W., Jr., Jiménez-Moreno, G., Reheis, M.C., and Simmons, K.R., 2009, this volume, A quarter-million years of paleoenvironmental change at Bear Lake, Utah and Idaho, in Rosenbaum, J.G., and Kaufman, D.S., eds., Paleoenvironments of Bear Lake, Utah and Idaho, and its catchment: Geological Society of America Special Paper 450, doi: 10.1130/2009.2450(14).
- King, J.W., and Channel, J.E.T., 1991, Sedimentary magnetism, environmental magnetism, and magnetostratigraphy: Reviews of Geophysics, v. 29, p. 358–370.
- Laabs, B.J.C., Munroe, J.S., Rosenbaum, J.G., Refsnider, K.A., Mickelson, D.M., Singer, B.S., and Caffee, M.W., 2007, Chronology of the Last Glacial Maximum in the Upper Bear River Basin, Utah: Arctic, Antarctic, and Alpine Research, v. 39, p. 537–548, doi: 10.1657/1523-0430(06-089) [LAABS]2.0.CO:2.
- Moore, D.M., and Reynolds, R.C., Jr., 1989, X-ray diffraction and identification and analysis of clay minerals: New York, Oxford University Press, 332 p.
- Oriel, S.S., and Platt, L.B., 1980, Geologic map of the Preston 1° × 2° quadrangle, southeastern Idaho and western Wyoming: U.S. Geological Survey, Miscellaneous Investigations Series Map I-1127, scale 1:250,000.
- Reheis, M.C., 2003, Dust deposition in Nevada, California, and Utah, 1984–2002: U.S. Geological Survey Open-File Report 03-138, <http://pubs.usgs.gov/of/2003/ofr-03-138/> (accessed June 2007).
- Reheis, M.C., 2006, 16-year record of dust deposition in southern Nevada and California, U.S.A.: Journal of Arid Environments, v. 67, p. 487–520, doi: 10.1016/j.jaridenv.2006.03.006.
- Reheis, M.C., and Kihl, R., 1995, Dust deposition in southern Nevada and California, 1984–1989—Relations to climate, source area, and source lithology: Journal of Geophysical Research (Atmospheres), v. 100, no. D5, p. 8893–8918, doi: 10.1029/94JD03245.
- Reheis, M.C., Laabs, J.C., and Kaufman, D.S., 2009, this volume, Geology and geomorphology of Bear Lake Valley and Upper Bear River, Utah and Idaho, in Rosenbaum, J.G., and Kaufman, D.S., eds., Paleoenvironments of Bear Lake, Utah and Idaho, and its catchment: Geological Society of America Special Paper 450, doi: 10.1130/2009.2450(02).
- Reynolds, R.L., and Rosenbaum, J.G., 2005, Magnetic mineralogy of sediments in Bear Lake and its watershed: Support for paleoenvironmental interpretations: U.S. Geological Survey Open-File Report 2005-1406, <http://pubs.usgs.gov/of/2005/1406/> (accessed June 2007).
- Reynolds, R.L., Tuttle, M.L., Rice, C., Fishman, N.S., Karachewski, J.A., and Sherman, D., 1994, Magnetization and geochemistry of greigite-bearing Cretaceous strata, North Slope basin, Alaska: American Journal of Science, v. 294, p. 485–528.
- Reynolds, R.L., Rosenbaum, J.G., Mazza, N., Rivers, W., and Luiszer, F., 1998, Sediment magnetic data (83 to 18 m depth) and XRF geochemical data (83 to 32 m depth) from lacustrine sediment in core OL-92 from Owens Lake, California, in Bischoff, J.L., ed., 1998, A high-resolution study of climate proxies in sediments from the last interglaciation at Owens Lake, California: Core OL-92: U.S. Geological Survey Open-File Report 98-132, 20 p.
- Reynolds, R.L., Sweetkind, D.S., and Axford, Y., 2001, An inexpensive magnetic mineral separator for fine-grained sediment: U.S. Geological Survey Open-File Report 01-281, 7 p.
- Reynolds, R.L., Rosenbaum, J.G., Rapp, J., Kerwin, M.W., Bradbury, J.P., Colman, S.C., and Adam, D., 2004, Record of late Pleistocene glaciation and deglaciation in the southern Cascade Range: I. Petrologic evidence from lacustrine sediment in Upper Klamath Lake, southern Oregon: Journal of Paleolimnology, v. 31, p. 217–233, doi: 10.1023/B:JOPL.0000019230.42575.03.
- Rose, N.L., Alliksaar, T., Bowman, J.J., Fott, J., Harlock, S., Punning, J.-M., St. Clair-Gribble, K., Vukic, J., and Watt, J., 1998, The FLAME Project: General discussion and overall conclusions: Water, Air, and Soil Pollution, v. 106, p. 329–351, doi: 10.1023/A:1005093313010.
- Rosenbaum, J.G., and Heil, C.W., Jr., 2009, this volume, The glacial/deglacial history of sedimentation in Bear Lake, Utah and Idaho, in Rosenbaum, J.G., and Kaufman, D.S., eds., Paleoenvironments of Bear Lake, Utah and Idaho, and its catchment: Geological Society of America Special Paper 450, doi: 10.1130/2009.2450(11).
- Rosenbaum, J.G., and Kaufman, D.S., 2009, this volume, Introduction to *Paleoenvironments of Bear Lake, Utah and Idaho, and its catchment*, in Rosenbaum, J.G., and Kaufman, D.S., eds., Paleoenvironments of Bear Lake, Utah and Idaho, and its catchment: Geological Society of America Special Paper 450, doi: 10.1130/2009.2450(00).
- Rosenbaum, J.G., and Reynolds, R.L., 2004, Record of late Pleistocene glaciation and deglaciation in the southern Cascade Range: II. Flux of glacial flour in a sediment core from Upper Klamath Lake, Oregon: Journal of Paleolimnology, v. 31, p. 235–252, doi: 10.1023/B:JOPL.0000019229.75336.7a.
- Smoot, J.P., 2009, this volume, Late Quaternary sedimentary features of Bear Lake, Utah and Idaho, in Rosenbaum, J.G., and Kaufman, D.S., eds., Paleoenvironments of Bear Lake, Utah and Idaho, and its catchment: Geological Society of America Special Paper 450, doi: 10.1130/2009.2450(03).
- Smoot, J.P., and Rosenbaum, J.G., 2009, this volume, Sedimentary constraints on late Quaternary lake-level fluctuations at Bear Lake, Utah and Idaho, in Rosenbaum, J.G., and Kaufman, D.S., eds., Paleoenvironments of Bear Lake, Utah and Idaho, and its catchment: Geological Society of America Special Paper 450, doi: 10.1130/2009.2450(12).

Geological Society of America Special Papers

Allogenic sedimentary components of Bear Lake, Utah and Idaho

Joseph G Rosenbaum, Walter E Dean, Richard L Reynolds, et al.

Geological Society of America Special Papers 2009;450; 145-168
doi:10.1130/2009.2450(06)

E-mail alerting services click www.gsapubs.org/cgi/alerts to receive free e-mail alerts when new articles cite this article

Subscribe click www.gsapubs.org/subscriptions to subscribe to Geological Society of America Special Papers

Permission request click www.geosociety.org/pubs/copyrt.htm#gsa to contact GSA.

Copyright not claimed on content prepared wholly by U.S. government employees within scope of their employment. Individual scientists are hereby granted permission, without fees or further requests to GSA, to use a single figure, a single table, and/or a brief paragraph of text in subsequent works and to make unlimited copies of items in GSA's journals for noncommercial use in classrooms to further education and science. This file may not be posted to any Web site, but authors may post the abstracts only of their articles on their own or their organization's Web site providing the posting includes a reference to the article's full citation. GSA provides this and other forums for the presentation of diverse opinions and positions by scientists worldwide, regardless of their race, citizenship, gender, religion, or political viewpoint. Opinions presented in this publication do not reflect official positions of the Society.

Notes